Search for exotic decays of a Higgs boson into undetectable particles and one or more photons

CMS Collaboration ; et al ; Canelli, M F ; Chiochia, V ; Kilminster, B ; Robmann, P

Abstract: A search is presented for exotic decays of a Higgs boson into undetectable particles and one or two isolated photons in pp collisions at a center-of-mass energy of 8 TeV. The data correspond to an integrated luminosity of up to 19.4 fb −1 collected with the CMS detector at the LHC. Higgs bosons produced in gluon–gluon fusion and in association with a Z boson are investigated, using models in which the Higgs boson decays into a gravitino and a neutralino or a pair of neutralinos, followed by the decay of the neutralino to a gravitino and a photon. The selected events are consistent with the background-only hypothesis, and limits are placed on the product of cross sections and branching fractions. Assuming a standard model Higgs boson production cross section, a 95% confidence level upper limit is set on the branching fraction of a 125 GeV Higgs boson decaying into undetectable particles and one or two isolated photons as a function of the neutralino mass. For this class of models and neutralino masses from 1 to 120 GeV an upper limit in the range of 7 to 13% is obtained. Further results are given as a function of the neutralino lifetime, and also for a range of Higgs boson masses.

DOI: https://doi.org/10.1016/j.physletb.2015.12.017

Originally published at:
CMS Collaboration; et al; Canelli, M F; Chiochia, V; Kilminster, B; Robmann, P (2016). Search for exotic decays of a Higgs boson into undetectable particles and one or more photons. Physics Letters B, 753:363-388.
DOI: https://doi.org/10.1016/j.physletb.2015.12.017

EUROPEAN ORGANIZATION FOR NUCLEAR RESEARCH (CERN)

CERN-PH-EP/2013-037
2015/12/31

CMS-HIG-14-025

Search for exotic decays of a Higgs boson into undetectable particles and one or more photons

The CMS Collaboration*

Abstract

A search is presented for exotic decays of a Higgs boson into undetectable particles and one or two isolated photons in pp collisions at a center-of-mass energy of 8 TeV. The data correspond to an integrated luminosity of up to 19.4 fb^{-1} collected with the CMS detector at the LHC. Higgs bosons produced in gluon-gluon fusion and in association with a Z boson are investigated, using models in which the Higgs boson decays into a gravitino and a neutralino or a pair of neutralinos, followed by the decay of the neutralino to a gravitino and a photon. The selected events are consistent with the background-only hypothesis, and limits are placed on the product of cross sections and branching fractions. Assuming a standard model Higgs boson production cross-section, a 95% confidence level upper limit is set on the branching fraction of a 125 GeV Higgs boson decaying into undetectable particles and one or two isolated photons as a function of the neutralino mass. For this class of models and neutralino masses from 1 to 120 GeV an upper limit in the range of 7 to 13% is obtained. Further results are given as a function of the neutralino lifetime, and also for a range of Higgs boson masses.

Published in Physics Letters B as `doi:10.1016/j.physletb.2015.12.017.`

*See Appendix A for the list of collaboration members

1 Introduction

The detailed studies of the properties of the observed Higgs boson [1–3] are key components of the LHC physics program. In the standard model (SM) and for a given mass of the Higgs boson, all properties of the Higgs boson are predicted. Physics beyond the SM (BSM) might lead to deviations from these predictions. Thus far, measurements of the Higgs bosons couplings to fermions and bosons and of the tensor structure of the Higgs boson interaction with electroweak gauge bosons show no significant deviations [4, 5] with respect to SM expectations.

Measurements of Higgs boson couplings performed for visible decay modes provide constraints on partial decay widths of the Higgs boson to BSM particles. Assuming that the couplings of the Higgs boson to W and Z bosons are smaller than the SM values, this indirect method provides an upper limit on the branching fraction of the 125 GeV Higgs boson to BSM particles of 57% at a 95% confidence level (CL) [4, 6]. An explicit search for BSM Higgs boson decays presents an alternative opportunity for the discovery of BSM physics. The observation of a sizable decay branching fraction of the Higgs boson to undetected (e.g. invisible or largely invisible) final states would be a clear sign of BSM physics and could provide a window on dark matter [7–10].

Several BSM models predict Higgs boson decays to undetectable particles and photons. In certain low-scale supersymmetry (SUSY) models, the Higgs bosons are allowed to decay into a gravitino ($\widetilde{\mathrm{G}}$) and a neutralino ($\widetilde{\chi}_1^0$) or a pair of neutralinos [11, 12]. The neutralino then decays into a photon and a gravitino, the lightest supersymmetric particle and dark matter candidate. Figure 1 shows Feynman diagrams for such decay chains of the Higgs boson (H) produced by gluon-gluon fusion (ggH) or in association with a Z boson decaying to charged leptons (ZH).

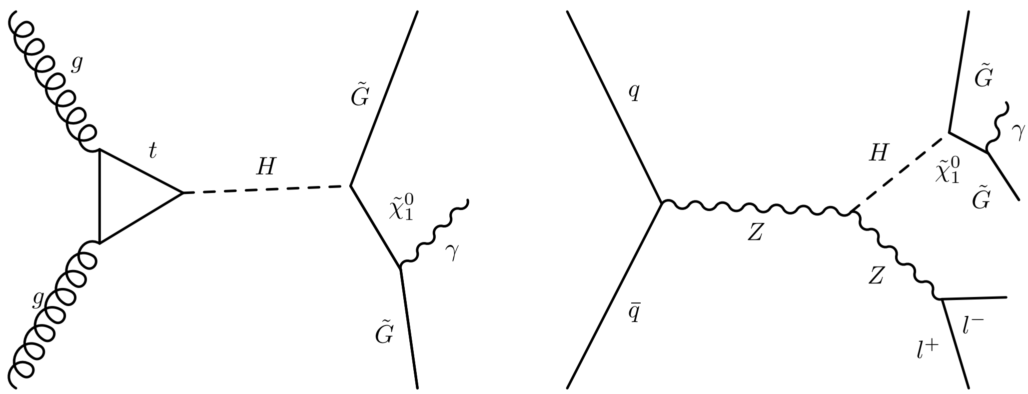

Figure 1: Feynman diagrams for the H $\rightarrow$ undetectable $+\ \gamma$ final state produced via ggH (left) and ZH (right).

As the gravitino in these models has a negligible mass [11, 12], the remaining parameter is the neutralino mass. If its mass is in the range $m_{\mathrm{H}}/2 < m_{\widetilde{\chi}_1^0} < m_{\mathrm{H}}$, with $m_{\mathrm{H}} = 125\,\mathrm{GeV}$ the mass of the observed Higgs boson, the branching fraction $\mathcal{B}(\mathrm{H} \rightarrow \widetilde{\chi}_1^0\widetilde{\mathrm{G}} \rightarrow \gamma\widetilde{\mathrm{G}}\widetilde{\mathrm{G}})$ can be large. For $m_{\widetilde{\chi}_1^0} < m_{\mathrm{H}}/2$, the decay $\mathrm{H} \rightarrow \widetilde{\chi}_1^0\widetilde{\chi}_1^0 \rightarrow \gamma\gamma\widetilde{\mathrm{G}}\widetilde{\mathrm{G}}$ is expected to dominate. The same discussion can be applied to heavy neutral Higgs bosons with masses larger than 125 GeV. The lifetime of the neutralino can be finite in some classes of BSM scenarios, leading to the production of one or more photons displaced from the primary interaction.

In the SM, the signature equivalent to the signal arises when the Higgs boson decays as $\mathrm{H} \rightarrow \mathrm{Z}\gamma \rightarrow \nu\bar{\nu}\gamma$ with a branching fraction of 3×10^{-4}. The decay $\mathrm{H} \rightarrow \mathrm{Z}\gamma$ has been studied in

$Z \to e^+e^-$ and $Z \to \mu^+\mu^-$ final states. Upper limits on the product of the cross section and branching fraction of about a factor of ten larger than the SM expectation have been set at the 95% CL [13, 14]. With the available dataset the search presented is not sensitive to this decay, but it is sensitive to enhancements in the Higgs boson decay rates to undetectable particles and photons arising from BSM physics.

Various background processes lead to the signal signatures and are estimated from simulation or from control samples in data. The dominant background processes are from γ+jets events and diboson events in the ggH and ZH search, respectively. Details of the background estimation techniques are discussed in Section 5. The strength of the ZH channel analysis is an almost background-free selection leading to a larger sensitivity in the model-dependent interpretation. While both the ggH and the ZH channels provide sensitivity to BSM Higgs boson signatures, the ggH channel allows a model-independent interpretation of the results.

This analysis presents a first search for decays of a scalar boson to undetectable particles and one or two isolated photons. The scalar boson is produced in ggH or in ZH. The data used correspond to an integrated luminosity of up to $19.4 \pm 0.5\,\mathrm{fb}^{-1}$ at a center-of-mass energy of $\sqrt{s} = 8$ TeV in 2012 collected with the CMS detector at the CERN LHC.

The results of the search are presented in terms of the low-scale SUSY breaking model for $m_{\mathrm{H}} = 125$ GeV and $m_{\tilde{\chi}^0_1}$ between 1 GeV and 120 GeV, and for m_{H} between 125 GeV and 400 GeV for the example case where $m_{\tilde{\chi}^0_1} = m_{\mathrm{H}} - 30$ GeV. The effect of a finite $\tilde{\chi}^0_1$ lifetime ($\tau_{\tilde{\chi}^0_1}$) is studied for the example case where $m_{\mathrm{H}} = 125$ GeV and $m_{\tilde{\chi}^0_1} = 95$ GeV.

2 The CMS experiment

The CMS detector, definitions of angular and spatial coordinates, and its performance can be found in Ref. [15]. The central feature of the CMS apparatus is a superconducting solenoid, of 6 m internal diameter, providing a magnetic field of 3.8 T. The field volume contains a silicon pixel and strip tracker, a crystal electromagnetic calorimeter (ECAL), and a brass and scintillator hadron calorimeter. Muons are measured in gas-ionization detectors embedded in the steel flux-return yoke of the magnet. The first level of the CMS trigger system, composed of specialized hardware processors, is designed to select the most interesting events within 3 μs, using information from the calorimeters and muon detectors. A high-level trigger processor farm is used to reduce the rate to a few hundred events per second before data storage.

A particle-flow algorithm [16, 17] is used to reconstruct all observable particles in the event. The algorithm combines all subdetector information to reconstruct individual particles and identify them as charged hadrons, neutral hadrons, photons, and leptons. The missing transverse energy vector $\vec{E}_{\mathrm{T}}^{\mathrm{miss}}$ is defined as the negative vector sum of the transverse momenta of all reconstructed particles (charged or neutral) in the event, with $E_{\mathrm{T}}^{\mathrm{miss}} = |\vec{E}_{\mathrm{T}}^{\mathrm{miss}}|$. Jets are reconstructed using the anti-k_{T} clustering algorithm [18] with a distance parameter of $R = 0.5$, as implemented in the FASTJET package [19, 20]. A multivariate selection is applied to separate jets from the primary interaction and those reconstructed due to energy deposits associated with pileup interactions [21]. The discrimination is based on the differences in the jet shapes, on the relative multiplicity of charged and neutral components, and on the different fraction of transverse momentum which is carried by the hardest components. Photon identification requirements and other procedures used in selecting events can be found in Section 4.

3 Data and simulation events

In the search for Higgs bosons produced in ggH, the trigger system requires the presence of one high transverse energy (E_{T}^{γ}) photon candidate and significant $E_{\mathrm{T}}^{\mathrm{miss}}$. The presence of a photon candidate with $E_{\mathrm{T}}^{\gamma} > 30\,\mathrm{GeV}$ is required within the ECAL barrel region ($|\eta^{\gamma}| < 1.44$). At the trigger level $E_{\mathrm{T}}^{\mathrm{miss}}$ is calculated from calorimeter information, and is not corrected for muons. A selection requirement of $E_{\mathrm{T}}^{\mathrm{miss}} > 25\,\mathrm{GeV}$ is applied. The efficiency of the trigger is monitored and measured with two control triggers for the photon and the $E_{\mathrm{T}}^{\mathrm{miss}}$ trigger requirement. The data recorded with this trigger correspond to an integrated luminosity of $7.4\,\mathrm{fb}^{-1}$ and were part of the CMS "data parking" program implemented for the last part of the data taking at $\sqrt{s} = 8\,\mathrm{TeV}$ in 2012. In that program, CMS recorded additional data with relaxed trigger requirements, planning for a delayed offline reconstruction in 2013 after the completion of the LHC Run 1.

For the search for Higgs bosons produced in ZH, collision events were collected using single-electron and single-muon triggers which require the presence of an isolated lepton with p_{T} in excess of 27 GeV and 24 GeV, respectively. Also a dilepton trigger was used, requiring two leptons with p_{T} thresholds of 17 GeV and 8 GeV. The luminosity integrated with these triggers at $\sqrt{s} = 8\,\mathrm{TeV}$ is $19.4\,\mathrm{fb}^{-1}$.

Several Monte Carlo (MC) event generators are used to simulate signal and background processes. The simulated samples are used to optimize the event selection, evaluate selection efficiencies and systematic uncertainties, and compute expected event yields. In all cases the MC samples are reweighted to match the trigger efficiency measured in data.

The Vγ, WZ, ZZ, VVV (where V represents W or Z bosons), Drell–Yan (DY) production of $\mathrm{q\overline{q}} \to \mathrm{Z}/\gamma^{*}$, and $\mathrm{q\overline{q}} \to \mathrm{W^{+}W^{-}}$ processes are generated with the MADGRAPH 5.1 event generator [22] at leading-order (LO), the $\mathrm{gg} \to \mathrm{W^{+}W^{-}}$ process is generated with the LO event generator GG2WW 3.1 [23], and the $\mathrm{t\bar{t}}$ and tW processes are generated with POWHEG 1.0 at next-to-leading-order (NLO). The signal samples are also produced with MADGRAPH. The cross sections at NLO or higher orders if available are used for a given process to renormalise the MC event generators. All processes are interfaced to the PYTHIA 6.4 generator [24] for parton shower and hadronization.

The CTEQ6L set of parton distribution functions (PDF) [25] is used for LO generators, while the CT10 [26] PDF set is used for NLO generators. For all processes, the detector response is simulated with a detailed description of the CMS detector, based on the GEANT4 package [27]. Additional pp interactions overlapping the event of interest in data, denoted as pileup events, are accounted for by simulating pp interactions with the PYTHIA generator and adding them to each MC sample. The MC samples are tuned to reproduce the distribution in the number of pileup events in data. The average number of pileup events is about 26 for the collected data used in the ggH channel, and is about 21 for the collected data used in the ZH channel.

4 Event selection

Two strategies are followed to isolate the Higgs boson events produced by ggH and by ZH from the background processes. The signal cross sections are several orders of magnitude smaller than the major reducible background processes, whose contributions are greatly reduced using the event selections described in the following sub-sections.

4.1 Event selection in the ggH channel

In the ggH channel, each selected event is required to have at least one photon candidate with $E_{\mathrm{T}}^{\gamma} > 45\,\mathrm{GeV}$ and $|\eta^{\gamma}| < 1.44$ using a cut-based selection [28, 29]. To reduce the SM backgrounds arising from the leptonic decays of W and Z bosons, a lepton veto is applied. Events are rejected if they have one or more electrons fulfilling a loose identification requirement [30] and $p_{\mathrm{T}}^{\mathrm{e}} > 10\,\mathrm{GeV}$ and $|\eta^{\mathrm{e}}| < 2.5$, excluding the transition region of $1.44 < |\eta^{\mathrm{e}}| \leq 1.57$ since the reconstruction of an electron object in this region is not optimal. Similarly, events containing muon candidates with $p_{\mathrm{T}}^{\mu} > 10\,\mathrm{GeV}$, $|\eta^{\mu}| < 2.1$, and well separated from the photon candidate requiring $\Delta R(\gamma,\mu) = \sqrt{(\Delta\eta)^2 + (\Delta\phi)^2} > 0.3$ (where the ϕ is azimuthal angle in radians), are rejected. In addition to the selection requirements described above, the $E_{\mathrm{T}}^{\mathrm{miss}}$ is required to be greater than 40 GeV. This level of selection is referred to as the preselection. Additional selection criteria are applied to search for new physics in either a quasi model-independent way or optimized for a SUSY benchmark model. In this channel jets can arise from initial-state radiation. For both search strategies jets are required to have $p_{\mathrm{T}}^{j} > 30\,\mathrm{GeV}$ and $|\eta^{j}| < 2.4$. These jets must not overlap with the photon candidate below $\Delta R(\gamma, \mathrm{jet}) < 0.5$.

In the model-independent analysis, events with two or more jets are rejected. For events with one jet the azimuthal angle between the photon and the jet ($\Delta\phi(\gamma, \mathrm{jet})$) is required to be smaller than 2.5. This selection requirement rejects the dominant γ+jet background, where the photon and the jet tend to be back to back in the transverse plane.

In the model-dependent analysis developed for SUSY scenarios, no requirement is applied on jet multiplicity. In order to minimize the contribution from processes such as γ+jets and multijet events, two methods are used for identifying events with mismeasured $E_{\mathrm{T}}^{\mathrm{miss}}$. The $E_{\mathrm{T}}^{\mathrm{miss}}$ significance method [31] takes account of reconstructed objects for each event and their known resolutions to compute an event-by-event estimate of the likelihood that the observed $E_{\mathrm{T}}^{\mathrm{miss}}$ is consistent with zero. In addition, a minimization method [29] constructs a χ^2 function of the form

$$\chi^2 = \sum_{i=\mathrm{objects}} \left(\frac{(p_{\mathrm{T}}^{\mathrm{reco}})_i - (\widetilde{p}_{\mathrm{T}})_i}{(\sigma_{p_{\mathrm{T}}})_i} \right)^2 + \left(\frac{\widetilde{E}_x^{\mathrm{miss}}}{\sigma_{E_x^{\mathrm{miss}}}} \right)^2 + \left(\frac{\widetilde{E}_y^{\mathrm{miss}}}{\sigma_{E_y^{\mathrm{miss}}}} \right)^2, \tag{1}$$

where $(p_{\mathrm{T}}^{\mathrm{reco}})_i$ are the scalar transverse momenta of the reconstructed objects, such as jets and photons that pass the above mentioned identification criteria, the $(\sigma_{p_{\mathrm{T}}})_i$ are the expected resolutions in each object, the $\sigma_{E_{x,y}^{miss}}$ are the resolution of the $E_{\mathrm{T}}^{\mathrm{miss}}$ projection along the x-axis and the y-axis, and the $(\widetilde{p}_{\mathrm{T}})_i$ are the free parameters allowed to vary in the minimization of the χ^2 function. The $\widetilde{\mathrm{E}}_{x,y}^{\mathrm{miss}}$ terms are functions of the free parameters $\widetilde{p}_{x,y}$,

$$\widetilde{E}_{x,y}^{\mathrm{miss}} = E_{x,y}^{\mathrm{miss,reco}} + \sum_{i=\mathrm{objects}} (p_{x,y}^{\mathrm{reco}})_i - (\widetilde{p}_{x,y})_i. \tag{2}$$

In events with no genuine $E_{\mathrm{T}}^{\mathrm{miss}}$, the mismeasured quantities are re-distributed back into the particle momenta, to minimize the χ^2 value. Events are rejected if the minimized $E_{\mathrm{T}}^{\mathrm{miss}}$ ($\widetilde{\mathrm{E}}_{\mathrm{T}}^{\mathrm{miss}}$) is less than 45 GeV and the chi-square probability is larger than 10^{-3}.

To further suppress multijet backgrounds, events are not considered if the scalar sum of the transverse momenta of the identified jets in the event (H_{T}) is greater than 100 GeV. An additional requirement is applied on the angle (α) between the beam direction and the major axis of the supercluster [28] in order to reject non-prompt photons that have showers elongated along the beam line.

Finally, the transverse mass, $m_{\mathrm{T}}^{\gamma E_{\mathrm{T}}^{\mathrm{miss}}} \equiv \sqrt{2E_{\mathrm{T}}^{\gamma}E_{\mathrm{T}}^{\mathrm{miss}}[1-\cos\Delta\phi(\gamma, E_{\mathrm{T}}^{\mathrm{miss}})]}$, formed by the photon candidate, $\vec{E}_{\mathrm{T}}^{\mathrm{miss}}$, and their opening angle, is required to be greater than 100 GeV. Photons from the continuum $\mathrm{Z}\gamma$ background have a harder spectrum than the photons resulting from the Higgs decay in the SUSY benchmark models considered. To further reduce the continuum $\mathrm{Z}\gamma$ background and for models with $m_{\mathrm{H}} = 125\,\mathrm{GeV}$ a cut of $E_{\mathrm{T}}^{\gamma} < 60\,\mathrm{GeV}$ is applied. For higher masses the cut is optimized depending on each mass hypothesis going from 60 GeV up to 200 GeV for $m_{\mathrm{H}} = 400\,\mathrm{GeV}$.

The list of selection criteria used in the model independent and the SUSY benchmark model analyses are given in Table 1, together with the cumulative efficiencies relative to the preselection for signal and background processes.

Table 1: Summary of ggH selection for both the quasi model-independent analysis and the analysis with the SUSY benchmark model with the cumulative efficiencies of the selection requirements relative to the preselection for $\mathrm{Z}\gamma \to \nu\bar{\nu}\gamma$, γ+jet and for a signal in a SUSY benchmark model with ggH production of a Higgs boson with mass 125 GeV decaying into a neutralino of mass 120 GeV and a photon.

Selection requirements	Model-independent		SUSY benchmark model		
	$\mathrm{Z}\gamma \to \nu\bar{\nu}\gamma$	γ+jet	$\mathrm{Z}\gamma \to \nu\bar{\nu}\gamma$	γ+jet	$m_{\tilde{\chi}_1^0} = 120\,\mathrm{GeV}$
Number of jets <2	0.909	0.769	—	—	—
$\Delta\phi(\gamma,\mathrm{jet}) < 2.5$ radians	0.834	0.262	—	—	—
Transverse mass > 100 GeV	—	—	0.867	0.292	0.829
$H_{\mathrm{T}} < 100\,\mathrm{GeV}$	—	—	0.785	0.188	0.804
$\widetilde{E}_{T}^{\mathrm{miss}} > 45\,\mathrm{GeV}$	—	—	0.761	0.071	0.743
$\mathrm{Prob}(\chi^2) < 10^{-3}$	—	—	0.626	0.033	0.467
$E_{\mathrm{T}}^{\mathrm{miss}}$ significance > 20	—	—	0.440	0.001	0.195
$\alpha > 1.2$	—	—	0.390	0.001	0.165
$E_{\mathrm{T}}^{\gamma} < 60\,\mathrm{GeV}$	—	—	0.074	0.0002	0.106

4.2 Event selection in the ZH channel

The leptonic decays of the Z boson, consisting of two oppositely charged same-flavor high-p_{T} isolated leptons ($\mathrm{e}^+\mathrm{e}^-$, $\mu^+\mu^-$), are used to tag the Higgs boson candidate events. Large missing transverse energy from the undetectable particles, at least one isolated high-E_{T} photon, and little or moderate jet activity are required to select the signal events.

The details of the lepton candidate selection and missing transverse energy reconstruction are given in Ref. [32]. In addition, photon requirements based on a multivariate selection discussed in Refs. [28, 33] have been used. The kinematic selection requires two leptons with $p_{\mathrm{T}} > 20\,\mathrm{GeV}$ and one photon with $E_{\mathrm{T}}^{\gamma} > 20\,\mathrm{GeV}$. Furthermore, the dilepton mass must be compatible with that of a Z boson within 15 GeV of the pole mass.

To reduce the background from WZ events, events are removed if an additional loosely identified lepton is reconstructed with $p_{\mathrm{T}} > 10\,\mathrm{GeV}$. To reject most of the top-quark background, an event is rejected if it passes the b-tagging selection (anti b-tagging) or if there is a selected jet with p_{T} larger than 30 GeV (jet veto). The b-tagging selection is based on the presence of a muon in the event from the semileptonic decay of a bottom-quark, and on the impact parameters of the constituent tracks in jets containing decays of bottom-quarks [34]. The set of b-tagging veto criteria retain about 95% of the light-quark jets, while rejecting about 70% of the b-jets.

The signal topology is characterized by a $\mathrm{Z}(\ell\ell)$ system with large transverse momentum balanced in the transverse plane by a $\vec{E}_{\mathrm{T}}^{\mathrm{miss}} + \vec{E}_{\mathrm{T}}^{\gamma}$ system from the Higgs boson decay. To reject background from $\mathrm{Z}\gamma$ and Z+jets events with misreconstructed $E_{\mathrm{T}}^{\mathrm{miss}}$ the azimuthal angle $\Delta\phi_{\ell\ell,\vec{E}_{\mathrm{T}}^{\mathrm{miss}}+\vec{E}_{\mathrm{T}}^{\gamma}}$ is required to be greater than 2.7 radians, the variable $|p_{\mathrm{T}}^{\vec{E}_{\mathrm{T}}^{\mathrm{miss}}+\vec{E}_{\mathrm{T}}^{\gamma}} - p_{\mathrm{T}}^{\ell\ell}|/p_{\mathrm{T}}^{\ell\ell}$ is required to be smaller than 0.5, and the azimuthal angle between the two leptons $\Delta\phi_{\ell\ell}$ is required to be smaller than 2.25 radians. Finally, $p_{\mathrm{T}}^{\ell\ell}$ is required to be larger than 60 GeV, and $E_{\mathrm{T}}^{\mathrm{miss}}$ is required to be larger than 60 GeV. A summary of the selection for the analysis is shown in Table 2.

The signal-to-background fraction depends on the $|\eta^{\gamma}|$, the pseudorapidity of the photon, with greater discrimination at lower values. To exploit this effect and improve sensitivity, the selected events are subdivided according to whether the photon is reconstructed in the barrel or endcap regions, as explained in Section 7.2.

Table 2: Summary of ZH selection.

Variable	Selection
Leptons	2 leptons, $p_{\mathrm{T}} > 20$ GeV
Photons	1 photon, $E_{\mathrm{T}}^{\gamma} > 20$ GeV
$\lvert m_{\ell\ell} - m_{\mathrm{Z}}\rvert$	$<$15 GeV
Anti b-tagging	applied
Jet veto	0 jets with $p_{\mathrm{T}}^{\mathrm{j}} > 30$ GeV
$\Delta\phi_{\ell\ell,\vec{E}_{\mathrm{T}}^{\mathrm{miss}}+\vec{E}_{\mathrm{T}}^{\gamma}}$	$>$2.7 radians
$\lvert p_{\mathrm{T}}^{\vec{E}_{\mathrm{T}}^{\mathrm{miss}}+\vec{E}_{\mathrm{T}}^{\gamma}} - p_{\mathrm{T}}^{\ell\ell}\rvert/p_{\mathrm{T}}^{\ell\ell}$	$<$0.50
$\Delta\phi_{\ell\ell}$	$<$2.25 radians
$p_{\mathrm{T}}^{\ell\ell}$	$>$60 GeV
$E_{\mathrm{T}}^{\mathrm{miss}}$	$>$60 GeV

5 Background estimation

The background estimation techniques and the composition of all backgrounds in the search with the ggH and ZH signatures are discussed below. The yield for the irreducible background from $\mathrm{H} \to \mathrm{Z}\gamma \to \nu\nu\gamma$ is negligible and is therefore ignored in the analysis.

5.1 Background estimation in the ggH channel

The dominant background for the $\gamma+E_{\mathrm{T}}^{\mathrm{miss}}$ signal in the ggH channel is the process γ+jet. Other SM backgrounds include $\mathrm{Z}\gamma \to \nu\bar{\nu}\gamma$, $\mathrm{W}\gamma$, $\mathrm{W} \to \mathrm{e}\nu$, $\mathrm{W} \to \mu\nu$, $\mathrm{W} \to \tau\nu$, multijet, and diphoton events. Background events that do not arise from pp collisions are also considered in the analysis. These backgrounds can be categorized broadly into three categories, as described below.

5.1.1 Background estimates from simulation

The γ+jet process surviving the various $E_{\mathrm{T}}^{\mathrm{miss}}$ selection requirements is one of the most significant backgrounds in this analysis due to the presence of an isolated photon and its large production cross section. The MC normalization of this background is corrected using control samples in data for two event classes, events without jets and those with one or more jets. The control samples in data are obtained using events collected with a prescaled single-photon trigger and with the $E_{\mathrm{T}}^{\mathrm{miss}}$ requirement reversed to ensure orthogonality to the signal phase space, where the contamination from other processes is minimal. Multiplicative correction factors (C) are obtained after normalizing the event yield in the simulation to match the data in the control region, separately for events with no jets ($C = 1.7$) and one or more jets ($C = 1.1$). These correction factors are used to normalize the simulated γ+jet event yield in the signal region. An uncertainty of 16% is obtained for these correction factors based on the difference between the corrected and uncorrected simulation and the relative fraction of no jet events (about 10% of the events in the control region) and one or more jet events. The background processes $\mathrm{Z}\gamma \to \ell\ell\gamma$ and $\mathrm{W} \to \mu\nu$ contribute only a small fraction of the total background prediction, due to the lepton veto applied at the preselection stage, and are modeled using simulated samples.

To take into account differences between data and simulation due to imperfect MC modeling, various scale factors (SF) are applied to correct the estimates from simulation. These SFs are defined by the ratio of the efficiency in data to the efficiency in simulation for a given selection. The SF for photon reconstruction and identification is estimated from $\mathrm{Z} \to \mathrm{e}^+\mathrm{e}^-$ decays [35] and is consistent with unity.

5.1.2 Background estimates from data

The contamination from jets misidentified as photons (jet $\to \gamma$) is estimated in a data control sample enriched with multijet events defined by $E_{\mathrm{T}}^{\mathrm{miss}} < 40\,\mathrm{GeV}$. This sample is used to measure the ratio of the number of candidates that pass the photon identification criteria to those failing the isolation requirements. The numerator of this ratio is further corrected for the photon contamination due to direct photon production using an isolation side band. The corrected ratio is applied to data events which pass the denominator selection and all other event requirements in the signal region.

The systematic uncertainty of this method is dominated by the choice of the isolation sideband, and is estimated to be 35% by changing the isolation criteria in the sideband region definition. The other sources of systematic uncertainty are determined by changing the $E_{\mathrm{T}}^{\mathrm{miss}}$ selection for the control region, and the loose identification requirements on the photons, all of which are found to be comparatively small.

Events with single electrons misidentified as photons (electron $\to \gamma$) are another major source of background. This background is estimated with a tag-and-probe method using $\mathrm{Z} \to \mathrm{e}^+\mathrm{e}^-$ events [36]. The efficiency to identify electrons ($\epsilon_{\gamma_\mathrm{e}}$) is estimated in the Z boson peak mass window of 60–120 GeV. The inefficiency ($1 - \epsilon_{\gamma_\mathrm{e}}$) is found to be $2.31 \pm 0.03\%$. The ratio $(1 - \epsilon_{\gamma_\mathrm{e}})/\epsilon_{\gamma_\mathrm{e}}$, which represents the electron misidentification rate, is applied to a sample where candidates are required to have hits in the pixel detector, and is used to estimate the contamination in the signal region. The misidentification rate is found to be dependent on the number of vertices reconstructed in the event and the number of tracks associated to the selected primary vertex. The difference in the final yields taking this dependence into account or neglecting it, using the inclusive measurement of $\epsilon_{\gamma_\mathrm{e}}$, is less than 5%.

5.1.3 Non-collision background estimates from data

The search is susceptible to contamination from non-collision backgrounds, which arise from cosmic ray interactions, spurious signals in the ECAL, and accelerator-induced secondary particles. The distribution of arrival-times of photons from these backgrounds is different to that of prompt photons produced in hard scattering. To quantify the contamination from these backgrounds a fit is performed to the candidate-time distribution using background distributions from the data [29]. The contamination due to out-of-time background contributions is found to be less than one percent of the total background and is therefore not included in the final event yield.

5.2 Background estimation in ZH channel

Processes that contribute significantly to the SM expectation in the ZH channel are listed below.

5.2.1 Non-resonant dilepton backgrounds

The contributions from W^+W^-, top-quark, W + jets, and $Z/\gamma^* \rightarrow \tau^+\tau^-$ processes are estimated by exploiting the lepton flavor symmetry in the final states of these processes [37]. The branching fraction to the $e^\pm\mu^\mp$ final state is twice that of the e^+e^- or $\mu^+\mu^-$ final states. Therefore, the $e^\pm\mu^\mp$ control region is used to extrapolate these backgrounds to the e^+e^- and $\mu^+\mu^-$ channels. The method considers differences between the electron and muon identification efficiencies. The data driven estimates agree well with the number of background events expected when applying the same method to simulation. The small difference between the prediction and the obtained value using simulated events is taken as a systematic uncertainty.

The limited number of simulated events is also considered as part of the systematic uncertainty. In summary, the total systematic uncertainty is about 75%. Only two events were selected in the data control region.

5.2.2 Resonant background with three leptons in the final state

The $WZ \rightarrow \ell\nu\ell\ell$ process dominates the resonant backgrounds with three leptons in the final state. The electron $\rightarrow \gamma$ misidentification rate is measured in $Z \rightarrow e^+e^-$ events by comparing the ratios of electron-electron versus electron-photon pairs in data and in simulation, as described in Section 5.1.2. The average misidentification rate is 1–2% with the larger values at higher $|\eta|^\gamma$.

5.2.3 Resonant background with two leptons in the final state

The $WZ \rightarrow \ell\nu\ell\ell$ process with failure to identify the lepton from W boson decays and the $ZZ \rightarrow 2\ell2\nu$ process dominate these types of events. The jet $\rightarrow \gamma$ misidentification rate is measured in a sample containing a muon and a photon. This sample is expected to be dominated by jets misidentified as photons, with some contamination from $W/Z\gamma$ events, which are subtracted in the study using the simulated prediction. The misidentification rate is similar to the obtained values in the ggH channel.

5.2.4 Resonant background with no genuine missing transverse energy

The background from $Z\gamma$ or Z + jets events is predicted by the simulation to be about 15% of the total background. Several data regions are studied to verify that the background is estimated correctly. A good agreement between data and simulation is found in all cases. A 50% uncertainty, the statistical uncertainty of the control region, is taken for these backgrounds estimated from simulation.

6 Summary of systematic uncertainties

Systematic uncertainties in the background estimates from control samples in data are described in Section 5. A summary of the systematic uncertainties considered in each channel are listed in Tables 3 and 4.

A common source of systematic uncertainty is associated with the measurement of the integrated luminosity, determined to 2.6% [38]. The uncertainties in the normalization of signal and simulation-based backgrounds are obtained by varying the renormalization and factorization scales, and the parton distribution functions [26, 39–43].

Because the model-independent and model-specific selections differ significantly in the ggH channel, the systematic uncertainties are evaluated separately for each selection. The photon energy scale uncertainty [28] of about 1% affects the signal and background predictions by 4% for the model specific selection and by 0.5% for the model-independent selection. Similarly, the jet energy scale uncertainty affects the signal and background predictions by 2–5% depending on the process and selection. After changing the photon or jet energy scales, the $E_{\mathrm{T}}^{\mathrm{miss}}$ is also recomputed. In addition, the systematic uncertainty associated with the jet energy resolution and unclustered energy scale are propagated to the $E_{\mathrm{T}}^{\mathrm{miss}}$ computation, and affect the signal and background predictions by 2–4%. As described in the previous section, a 16% uncertainty is applied to the γ+jet normalization due to the difference in the jet multiplicity distribution between the data and background predictions in the γ+jet control region. The uncertainty due to the pileup modeling is found to be 1%, and is estimated by shifting the central value of the total inelastic cross section within its uncertainty.

Table 3: Summary of all relative systematic uncertainties in percent for the signal and background estimates for the Higgs model (model-independent in parenthesis) selection in the ggH analysis.

Source	Signal	Jet$\rightarrow\gamma$	Electron$\rightarrow\gamma$	γ + jet	Z$\nu\nu\gamma$	Wγ
PDF	10 (0)	—	—	—	4 (4)	4 (4)
Integrated luminosity	2.6 (2.6)	—	—	2.6 (2.6)	2.6 (2.6)	2.6 (2.6)
Photon efficiency	3 (3)	—	—	3 (3)	3 (3)	3 (3)
Photon energy scale $\pm$ 1 %	4 (0.5)	—	—	4 (0.5)	4 (0.5)	4 (0.5)
$E_{\mathrm{T}}^{\mathrm{miss}}$ energy scale	4 (2)	—	—	4 (2)	4 (2)	4 (2)
Jet energy scale	3 (2)	—	—	5 (5)	3 (2)	3 (2)
Pileup	1 (1)	—	—	1 (1)	1 (1)	1 (1)
Z$\nu\nu\gamma$ normalization	—	—	—	—	3 (3)	—
γ + jet normalization	—	—	—	16 (16)	—	—
Wγ normalization	—	—	—	—	—	3 (3)
Jet $\rightarrow\gamma$	—	35 (35)	—	—	—	—
Electron $\rightarrow\gamma$	—	—	6 (6)	—	—	—

In the ZH channel, lepton-reconstruction and identification scale factors are measured using a control sample of $Z/\gamma^* \rightarrow \ell^+\ell^-$ events in the Z peak region [36]. The associated uncertainty is about 2% per lepton. The photon identification uncertainty is taken to be 3% [33]. The effect of uncertainties in jet-energy scale and $E_{\mathrm{T}}^{\mathrm{miss}}$ on the analysis is also considered. The uncertainty in the b-tagging efficiency is estimated to be about 0.7% comparing inclusive $Z/\gamma^* \rightarrow \ell^+\ell^-$ samples in data and simulation. The total uncertainty in the background estimates in the signal region is 36%, which is dominated by the statistical uncertainties in the data control samples from which they are derived.

The impact of the systematic uncertainties in the ggH channel is relatively important: the sensitivity is increased by about 50% if all the systematic uncertainties are removed, where the normalization uncertainties on the γ + jet and jet $\rightarrow\gamma$ background processes dominate. The ZH channel is limited by the statistical uncertainty, and the effect of the systematic uncertainties reduce the sensitivity by less than 10%.

Table 4: Summary of relative systematic uncertainties in percent for the signal and background estimates in the ZH analysis.

Source	ZH	$Z\gamma$ or $Z+\text{jets}$	WZ	ZZ	WW + top-quark
Integrated luminosity	2.6	—	2.6	2.6	—
Lepton efficiency	3.6	—	3.6	3.6	—
Photon efficiency	3.0	—	—	—	—
Momentum resolution	0.5	—	1	1	—
$E_{\mathrm{T}}^{\text{miss}}$ energy scale	0.5	—	0.6	0.1	—
Jet energy scale	2	—	4	4	—
b-tagging	0.7	—	0.7	0.7	—
Underlying event	3	—	—	—	—
PDF	7.1	—	6.3	7.7	—
Renorm. and factor. scales	7.0	—	10.7	6.5	—
$Z/\gamma^* \to \ell^+\ell^-$ normalization	—	50	—	—	—
Non-resonant dilepton bkg. norm.	—	—	—	—	70
Jet $\to \gamma$	—	—	30	30	—
Electron $\to \gamma$	—	—	10	10	—
Amount of simulated events	3.5	60	10	30	40

Correlations between systematic uncertainties in the two channels are taken into account. In particular, the main sources of correlated systematic uncertainties are those in the experimental measurements such as the integrated luminosity, photon identification, the jet energy scale, and missing transverse energy resolution. All other systematic uncertainties are uncorrelated between them given the different signal and background processes.

7 Results

The results from the two searches and their combination are reported in this section. In the absence of deviations from the standard model predictions, the modified frequentist method, $\mathrm{CL_s}$ [44–46], is used to define the exclusion limits.

7.1 Model-independent results in the ggH channel

Because of the variety of possible BSM signals that could contribute to this final state, the results are presented for a signal with the model-independent selection described in Section 4. The total number of observed events and the estimated SM backgrounds are summarized in Table 5, and found to be compatible within their uncertainties. Figure 2 shows the $m_{\mathrm{T}}^{\gamma E_{\mathrm{T}}^{\text{miss}}}$ and $E_{\mathrm{T}}^{\text{miss}}$ distributions for the model-independent selection.

Figure 3 shows the observed and expected model-independent 95% CL upper limits for the ggH analysis on the product of cross section, acceptance, and efficiency for $m_{\mathrm{T}}^{\gamma E_{\mathrm{T}}^{\text{miss}}} > 100\,\text{GeV}$, as a function of $E_{\mathrm{T}}^{\text{miss}}$ threshold.

7.2 Model-specific results in the ggH channel

Imposing the model-specific selection described in Section 4 for the ggH channel, 1296 events are selected in data with a total estimated background of 1232 ± 188. The yields for this selection are shown in Table 6 and estimated for Higgs boson decays ($\mathrm{H} \to \widetilde{\mathrm{G}}\widetilde{\chi}_1^0, \widetilde{\chi}_1^0 \to \widetilde{\mathrm{G}}\gamma$) assuming the ggH production rate for SM Higgs bosons and a 100% branching fraction for this decay. Figure 4 shows the transverse energy distribution of photons for data, the background

Table 5: Observed yields and background estimates at 8 TeV in the ggH channel after the model-independent selection. Statistical and systematic uncertainties are shown.

Process	Event yields
γ+ jets	$(313 \pm 50) \times 10^3$
jet $\to \gamma$	$(910 \pm 320) \times 10^2$
e $\to \gamma$	10350 ± 620
$\mathrm{W}(\to \ell\nu) + \gamma$	2239 ± 111
$\mathrm{Z}(\to \nu\bar{\nu}) + \gamma$	2050 ± 102
Other	1809 ± 91
Total background	$(420 \pm 82) \times 10^3$
Data	442×10^3

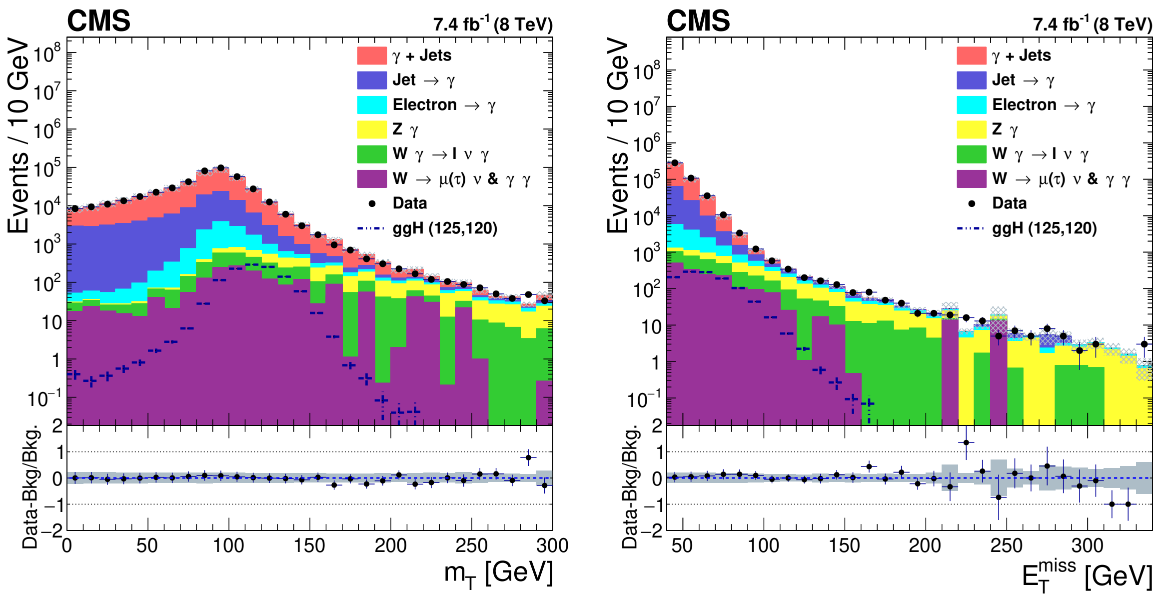

Figure 2: The $m_{\mathrm{T}}^{\gamma E_{\mathrm{T}}^{\mathrm{miss}}}$ and $E_{\mathrm{T}}^{\mathrm{miss}}$ distributions for data, background estimates, and signal after the model-independent selection for the ggH channel. The bottom panels in each plot show the ratio of (data - background)/background and the gray band includes both the statistical and systematic uncertainties in the background prediction. The signal is shown for $m_{\mathrm{H}} = 125\,\mathrm{GeV}$ and $m_{\tilde{\chi}_1^0} = 120\,\mathrm{GeV}$ and a 100% branching fraction.

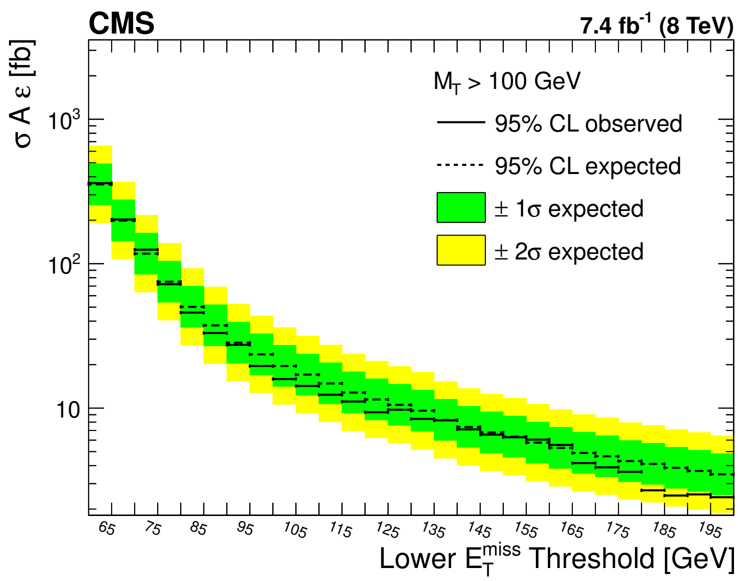

Figure 3: The expected and observed 95% CL upper limit on the product of cross section, acceptance, and efficiency ($\sigma(\mathrm{pp} \to \gamma + E_{\mathrm{T}}^{\mathrm{miss}}) A\epsilon$) for $m_{\mathrm{T}}^{\gamma E_{\mathrm{T}}^{\mathrm{miss}}} > 100\,\mathrm{GeV}$, as function of the $E_{\mathrm{T}}^{\mathrm{miss}}$ threshold for the ggH channel.

estimates, and signal after the model-dependent selection, except the upper selection on the photon, for the ggH channel.

7.3 Results in the ZH channel and combinations

A total of four events are selected with the search in ZH. The background yield is estimated to 4.1 ± 1.8. The numbers of observed and expected events are shown in Table 7. The signal model assumes a SM ZH production rate and a 100% branching fraction to undetectable particles and one or two photons. The expected signal yield is larger for cases where $m_{\widetilde{\chi}_1^0}$ is smaller than $m_{\mathrm{H}}/2$ since there are two photons in the final state ($\mathrm{H} \to \widetilde{\chi}_1^0\widetilde{\chi}_1^0 \to \gamma\gamma\widetilde{\mathrm{G}}\widetilde{\mathrm{G}}$), and as a result the sensitivity improves for smaller masses. Good agreement between the data and the background prediction is observed. The transverse mass, $m_{\mathrm{T}}^{\ell\ell E_{\mathrm{T}}^{\mathrm{miss}}} \equiv \sqrt{2p_{\mathrm{T}}^{\ell\ell} p_{\mathrm{T}}^{\vec{E}_{\mathrm{T}}^{\mathrm{miss}}+\vec{E}_{\mathrm{T}}^{\gamma}}[1 - \cos(\Delta\phi_{\ell\ell,\vec{E}_{\mathrm{T}}^{\mathrm{miss}}+\vec{E}_{\mathrm{T}}^{\gamma}})]}$, and $|\eta^{\gamma}|$ distributions discriminate signal and background and are shown in Figure 5 at the final step of the selection.

The 95% CL upper limits are extracted from counting experiments in three categories: the model-specific selection in the ggH channel, and photons identified in the barrel and the endcap calorimeters for the ZH channel. Results are combined using a binned-likelihood method. The 95% CL upper limits on $(\sigma\,\mathcal{B})/\sigma_{SM}$, where σ_{SM} is the cross section for the SM Higgs boson, are evaluated for different mass values of $\widetilde{\chi}_1^0$ ranging from 1 GeV to 120 GeV for the individual searches and their combination and are shown in Figure 6. The upper limits for $m_{\widetilde{\chi}_1^0} < m_{\mathrm{H}}/2$ are not shown for the ggH channel because the sensitivity is very low due to the combination kinematic properties and the corresponding selection; in particular the $E_{\mathrm{T}}^{\mathrm{miss}}$ and photon p_{T} values tend to be outside the selected ranges. A 95% CL upper limit on the branching fraction of 10% is set for a neutralino mass of 95 GeV.

Expected and observed limits are also shown for the decay of possible heavier scalar Higgs bosons as a function of the Higgs boson mass in Figure 7. The requirement on E_{T}^{γ} used in the ggH channel is removed. A lower threshold on E_{T}^{γ} is added, optimized to maximize the

Table 6: Observed yields, background estimates, and signal predictions at 8 TeV in the ggH channel for different values of the $m_{\tilde{\chi}_1^0}$ and for different $c\tau_{\tilde{\chi}_1^0}$ of the $\tilde{\chi}_1^0$. These correspond to $\mathcal{B}(\mathrm{H} \to \text{undetectable} + \gamma) = 100\%$, assuming the SM cross section at the given m_H hypothesis. The combination of statistical and systematic uncertainties is shown for the yields.

Process	Event yields
$\mathrm{ggH}(m_\mathrm{H} = 125\,\mathrm{GeV}, m_{\tilde{\chi}_1^0} = 65\,\mathrm{GeV})$	653 ± 77
$\mathrm{ggH}(m_\mathrm{H} = 125\,\mathrm{GeV}, m_{\tilde{\chi}_1^0} = 95\,\mathrm{GeV})$	1158 ± 137
$\mathrm{ggH}(m_\mathrm{H} = 125\,\mathrm{GeV}, m_{\tilde{\chi}_1^0} = 120\,\mathrm{GeV})$	2935 ± 349
$\mathrm{ggH}(m_\mathrm{H} = 125\,\mathrm{GeV}, m_{\tilde{\chi}_1^0} = 95\,\mathrm{GeV})\ c\tau_{\tilde{\chi}_1^0} = 100\,\mathrm{mm}$	983 ± 116
$\mathrm{ggH}(m_\mathrm{H} = 125\,\mathrm{GeV}, m_{\tilde{\chi}_1^0} = 95\,\mathrm{GeV})\ c\tau_{\tilde{\chi}_1^0} = 1000\,\mathrm{mm}$	463 ± 55
$\mathrm{ggH}(m_\mathrm{H} = 125\,\mathrm{GeV}, m_{\tilde{\chi}_1^0} = 95\,\mathrm{GeV})\ c\tau_{\tilde{\chi}_1^0} = 10000\,\mathrm{mm}$	83 ± 10
$\mathrm{ggH}(m_\mathrm{H} = 150\,\mathrm{GeV}, m_{\tilde{\chi}_1^0} = 120\,\mathrm{GeV})$	4160 ± 491
$\mathrm{ggH}(m_\mathrm{H} = 200\,\mathrm{GeV}, m_{\tilde{\chi}_1^0} = 170\,\mathrm{GeV})$	5963 ± 704
$\mathrm{ggH}(m_\mathrm{H} = 300\,\mathrm{GeV}, m_{\tilde{\chi}_1^0} = 270\,\mathrm{GeV})$	5152 ± 608
$\mathrm{ggH}(m_\mathrm{H} = 400\,\mathrm{GeV}, m_{\tilde{\chi}_1^0} = 370\,\mathrm{GeV})$	4057 ± 479
$\gamma +$ jets	179 ± 28
jet $\to \gamma$	269 ± 94
$\mathrm{e} \to \gamma$	355 ± 28
$\mathrm{W}(\to \ell\nu) + \gamma$	154 ± 15
$\mathrm{Z}(\to \nu\bar{\nu}) + \gamma$	182 ± 13
Other	91 ± 10
Total background	1232 ± 188
Data	1296

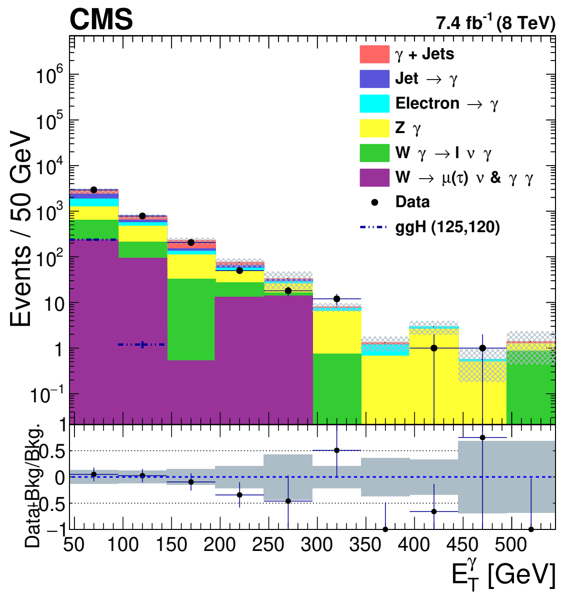

Figure 4: The transverse energy distribution of photons for data, the background estimates, and signal after the model-dependent selection (except the upper selection on the photon) for the ggH channel. The bottom panel shows the ratio of (data - background)/background and the gray band includes both the statistical and systematic uncertainties in the background prediction. The signal is shown for $m_\mathrm{H} = 125\,\mathrm{GeV}$ and $m_{\tilde{\chi}_1^0} = 120\,\mathrm{GeV}$.

Table 7: Observed yields, background estimates, and signal predictions at 8 TeV in the ZH channel for different values of the $m_{\widetilde{\chi}^0_1}$ and for different $c\tau_{\widetilde{\chi}^0_1}$ of the $\widetilde{\chi}^0_1$. The signal predictions correspond to $\mathcal{B}(\mathrm{H} \to \text{ undetectable} + \gamma)$ =100% assuming the SM ZH cross section at the given m_{H} hypothesis. The combination of statistical and systematic uncertainties is shown for the yields.

Process	Event yields
$\mathrm{ZH}(m_{\mathrm{H}} = 125\,\mathrm{GeV}, m_{\widetilde{\chi}^0_1} = 1\,\mathrm{GeV})$	69.2 ± 8.4
$\mathrm{ZH}(m_{\mathrm{H}} = 125\,\mathrm{GeV}, m_{\widetilde{\chi}^0_1} = 10\,\mathrm{GeV})$	68.6 ± 8.4
$\mathrm{ZH}(m_{\mathrm{H}} = 125\,\mathrm{GeV}, m_{\widetilde{\chi}^0_1} = 30\,\mathrm{GeV})$	53.5 ± 6.5
$\mathrm{ZH}(m_{\mathrm{H}} = 125\,\mathrm{GeV}, m_{\widetilde{\chi}^0_1} = 60\,\mathrm{GeV})$	47.7 ± 5.8
$\mathrm{ZH}(m_{\mathrm{H}} = 125\,\mathrm{GeV}, m_{\widetilde{\chi}^0_1} = 65\,\mathrm{GeV})$	40.0 ± 4.9
$\mathrm{ZH}(m_{\mathrm{H}} = 125\,\mathrm{GeV}, m_{\widetilde{\chi}^0_1} = 95\,\mathrm{GeV})$	40.3 ± 4.9
$\mathrm{ZH}(m_{\mathrm{H}} = 125\,\mathrm{GeV}, m_{\widetilde{\chi}^0_1} = 120\,\mathrm{GeV})$	39.0 ± 4.8
$\mathrm{ZH}(m_{\mathrm{H}} = 125\,\mathrm{GeV}, m_{\widetilde{\chi}^0_1} = 95\,\mathrm{GeV})\ c\tau_{\widetilde{\chi}^0_1} = 100\,\mathrm{mm}$	39.3 ± 4.8
$\mathrm{ZH}(m_{\mathrm{H}} = 125\,\mathrm{GeV}, m_{\widetilde{\chi}^0_1} = 95\,\mathrm{GeV})\ c\tau_{\widetilde{\chi}^0_1} = 1000\,\mathrm{mm}$	17.6 ± 2.2
$\mathrm{ZH}(m_{\mathrm{H}} = 125\,\mathrm{GeV}, m_{\widetilde{\chi}^0_1} = 95\,\mathrm{GeV})\ c\tau_{\widetilde{\chi}^0_1} = 10000\,\mathrm{mm}$	2.6 ± 0.3
$\mathrm{ZH}(m_{\mathrm{H}} = 200\,\mathrm{GeV}, m_{\widetilde{\chi}^0_1} = 170\,\mathrm{GeV})$	13.1 ± 1.6
$\mathrm{ZH}(m_{\mathrm{H}} = 300\,\mathrm{GeV}, m_{\widetilde{\chi}^0_1} = 270\,\mathrm{GeV})$	3.5 ± 0.4
$\mathrm{ZH}(m_{\mathrm{H}} = 400\,\mathrm{GeV}, m_{\widetilde{\chi}^0_1} = 370\,\mathrm{GeV})$	1.2 ± 0.1
$\mathrm{Z}\gamma + \mathrm{Z} + \text{jets}$	0.6 ± 0.4
WZ	1.2 ± 0.3
ZZ	0.3 ± 0.1
WW + top-quark	2.0 ± 1.7
Total background	4.1 ± 1.8
Data	4

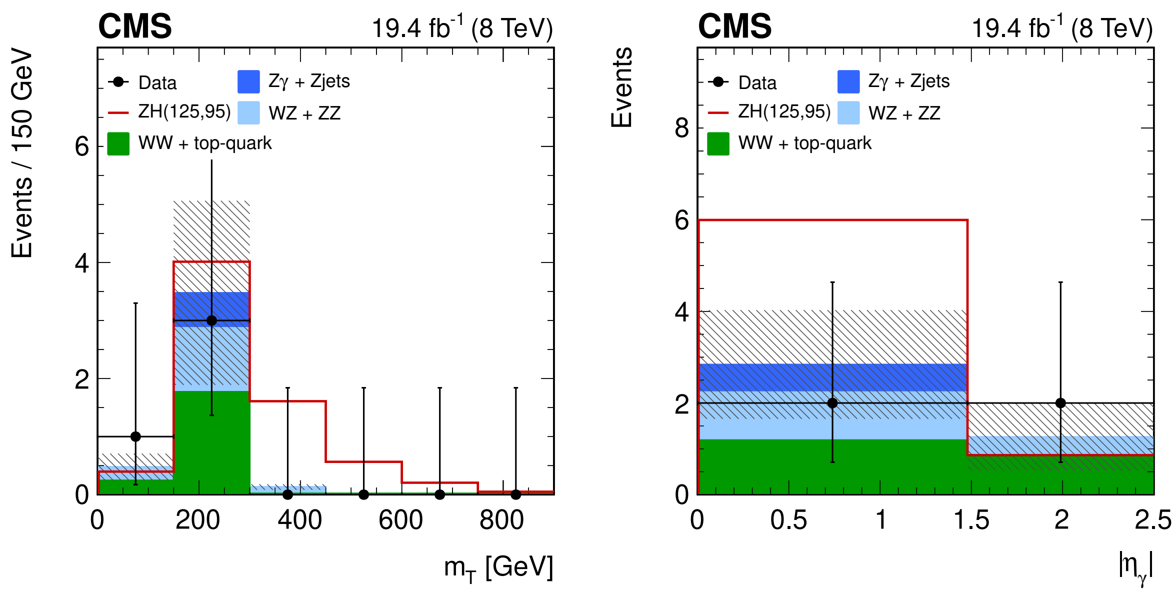

Figure 5: Distributions in signal where $m_{\mathrm{H}} = 125\,\mathrm{GeV}$ and $m_{\tilde{\chi}^0_1} = 95\,\mathrm{GeV}$, backgrounds and data for $m_{\mathrm{T}}^{\ell\ell E_{\mathrm{T}}^{\mathrm{miss}}}$ (left) and $|\eta^{\gamma}|$ (right) after applying all requirements. The uncertainty band for the backgrounds includes both statistical and systematic uncertainties. The signal model assumes a SM ZH production rate for a Higgs boson with $m_{\mathrm{H}} = 125\,\mathrm{GeV}$ and a 10% branching fraction.

sensitivity for each mass hypothesis. A combination of the two channels is not performed because the assumption of a common SM Higgs boson cross section is not justified.

As discussed in the introduction, some BSM models predict $\tilde{\chi}^0_1$ neutralinos with sizable lifetimes. The performance of the searches has been evaluated for finite lifetimes without modifying the analysis strategy. The expected and observed limits are shown in Figure 8 as function of $c\tau_{\tilde{\chi}^0_1}$. The results are shown for $m_{\mathrm{H}} = 125\,\mathrm{GeV}$ and $m_{\tilde{\chi}^0_1} = 95\,\mathrm{GeV}$. As seen in Tables 6 and 7, the selection efficiency is roughly constant for values of $c\tau_{\tilde{\chi}^0_1}$ less than 10 cm, and drops rapidly for larger values. The default timing criteria applied in the ECAL energy reconstruction are the cause for the decrease in the efficiency. In particular, there is a requirement of a maximum of 3 ns on the photon arrival time relative to the nominal time-of-flight for prompt photons. The delayed arrival time of the photon can be caused by a kink in the trajectory or by a lower velocity of the neutralino.

8 Summary

A search is presented for exotic decays of a Higgs boson into undetectable particles and one or two isolated photons in pp collisions at a center-of-mass energy of 8 TeV. The data correspond to an integrated luminosity of up to 19.4 fb^{-1} collected with the CMS detector at the LHC. Higgs bosons produced in gluon-gluon fusion or in association with a Z boson are investigated. Models including Higgs boson decays into a gravitino and a neutralino or a pair of neutralinos, followed by the neutralino decay to a gravitino and a photon, are tested. The measurements for the selected events in data are consistent with the background only hypothesis, and the results are interpreted as limits on the product of cross sections and branching fractions. Assuming a standard model Higgs production cross-section, a 95% CL upper limit is set on the branching

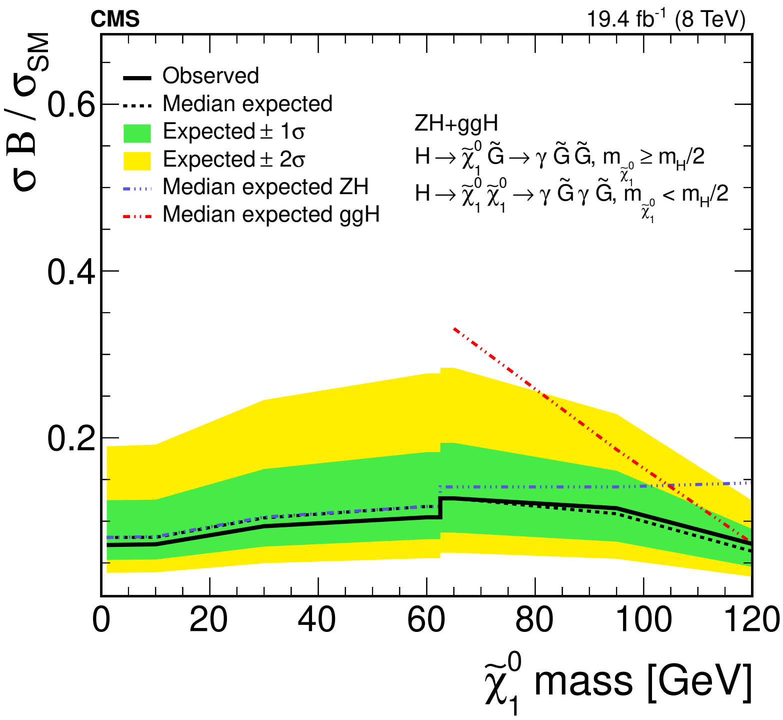

Figure 6: Expected and observed 95% CL upper limits on $\sigma \mathcal{B}/\sigma_{\mathrm{SM}}$ for $m_{\mathrm{H}} = 125\,\mathrm{GeV}$ as a function of $m_{\tilde{\chi}_1^0}$ assuming the SM Higgs boson cross sections, for the ZH and ggH channels and their combination, with $\mathcal{B} \equiv \mathcal{B}(\mathrm{H} \to \tilde{\chi}_1^0\tilde{\chi}_1^0)\,\mathcal{B}(\tilde{\chi}_1^0 \to \tilde{\mathrm{G}} + \gamma)^2$ for $m_{\tilde{\chi}_1^0} < m_{\mathrm{H}}/2$ and $\mathcal{B} \equiv \mathcal{B}(\mathrm{H} \to \tilde{\chi}_1^0\tilde{\mathrm{G}})\,\mathcal{B}(\tilde{\chi}_1^0 \to \tilde{\mathrm{G}} + \gamma)$ for $m_{\tilde{\chi}_1^0} \geq m_{\mathrm{H}}/2$.

fraction of a 125 GeV Higgs boson decaying into undetectable particles and one or two isolated photons as a function of the neutralino mass. For neutralino masses from 1 to 120 GeV an upper limit in the range of 7 to 13% is obtained. Further results are given as a function of the neutralino lifetime, and also for a range of Higgs boson masses.

Acknowledgments

We congratulate our colleagues in the CERN accelerator departments for the excellent performance of the LHC and thank the technical and administrative staffs at CERN and at other CMS institutes for their contributions to the success of the CMS effort. In addition, we gratefully acknowledge the computing centers and personnel of the Worldwide LHC Computing Grid for delivering so effectively the computing infrastructure essential to our analyses. Finally, we acknowledge the enduring support for the construction and operation of the LHC and the CMS detector provided by the following funding agencies: BMWFW and FWF (Austria); FNRS and FWO (Belgium); CNPq, CAPES, FAPERJ, and FAPESP (Brazil); MES (Bulgaria); CERN; CAS, MoST, and NSFC (China); COLCIENCIAS (Colombia); MSES and CSF (Croatia); RPF (Cyprus); MoER, ERC IUT and ERDF (Estonia); Academy of Finland, MEC, and HIP (Finland); CEA and CNRS/IN2P3 (France); BMBF, DFG, and HGF (Germany); GSRT (Greece); OTKA and NIH (Hungary); DAE and DST (India); IPM (Iran); SFI (Ireland); INFN (Italy); MSIP and NRF (Republic of Korea); LAS (Lithuania); MOE and UM (Malaysia); CINVESTAV, CONACYT, SEP, and UASLP-FAI (Mexico); MBIE (New Zealand); PAEC (Pakistan); MSHE and NSC (Poland); FCT (Portugal); JINR (Dubna); MON, RosAtom, RAS and RFBR (Russia); MESTD (Serbia);

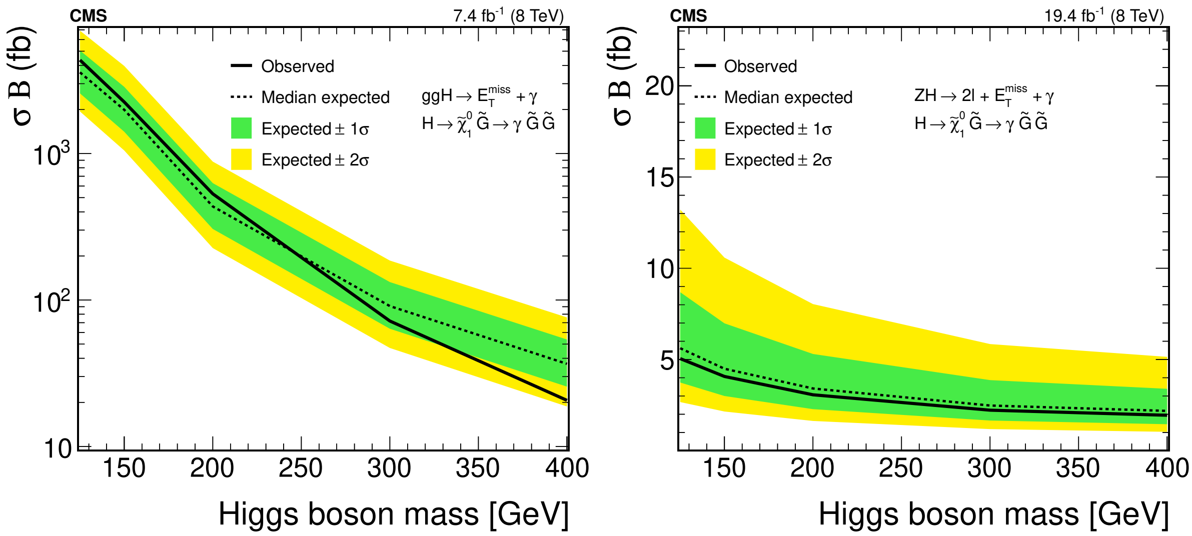

Figure 7: Expected and observed 95% CL upper limits on $\sigma_{gg\to\mathrm{H}}\,\mathcal{B}$ as a function of the Higgs boson mass with $m_{\tilde{\chi}_1^0} = m_\mathrm{H} - 30\,\mathrm{GeV}$ in ggH channel (left) and in the ZH channel (right).

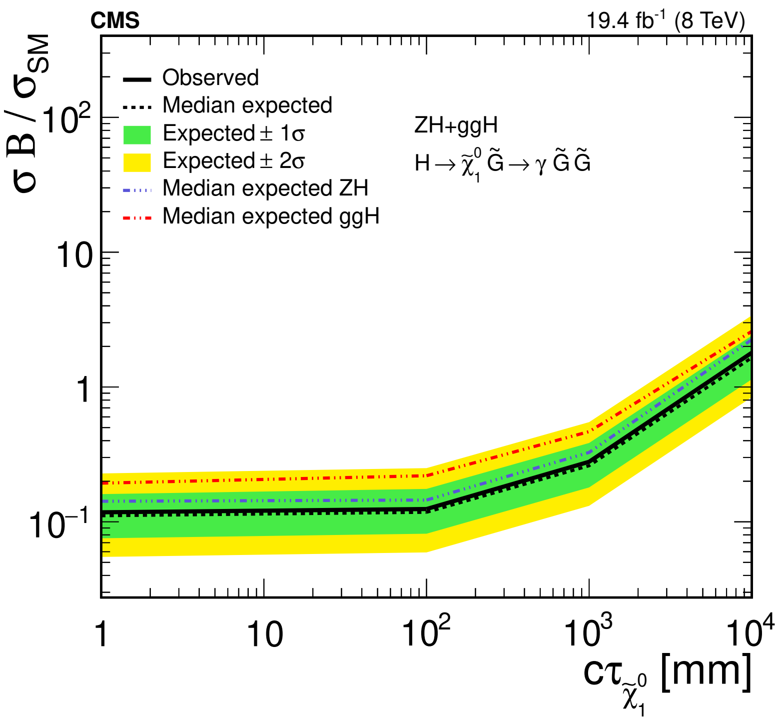

Figure 8: Expected and observed 95% CL upper limits on $\sigma_\mathrm{H}\,\mathcal{B}$ as a function of $c\tau_{\tilde{\chi}_1^0}$ for $m_\mathrm{H} = 125\,\mathrm{GeV}$ and $m_{\tilde{\chi}_1^0} = 95\,\mathrm{GeV}$, where $\mathcal{B} \equiv \mathcal{B}(\mathrm{H} \to \tilde{\chi}_1^0\tilde{\mathrm{G}})\,\mathcal{B}(\tilde{\chi}_1^0 \to \tilde{\mathrm{G}} + \gamma)$.

SEIDI and CPAN (Spain); Swiss Funding Agencies (Switzerland); MST (Taipei); ThEPCenter, IPST, STAR and NSTDA (Thailand); TUBITAK and TAEK (Turkey); NASU and SFFR (Ukraine); STFC (United Kingdom); DOE and NSF (USA).

Individuals have received support from the Marie-Curie program and the European Research Council and EPLANET (European Union); the Leventis Foundation; the A. P. Sloan Foundation; the Alexander von Humboldt Foundation; the Belgian Federal Science Policy Office; the Fonds pour la Formation à la Recherche dans l'Industrie et dans l'Agriculture (FRIA-Belgium); the Agentschap voor Innovatie door Wetenschap en Technologie (IWT-Belgium); the Ministry of Education, Youth and Sports (MEYS) of the Czech Republic; the Council of Science and Industrial Research, India; the HOMING PLUS program of the Foundation for Polish Science, cofinanced from European Union, Regional Development Fund; the Compagnia di San Paolo (Torino); the Consorzio per la Fisica (Trieste); MIUR project 20108T4XTM (Italy); the Thalis and Aristeia programs cofinanced by EU-ESF and the Greek NSRF; the National Priorities Research Program by Qatar National Research Fund; and Rachadapisek Sompot Fund for Postdoctoral Fellowship, Chulalongkorn University (Thailand).

References

[1] ATLAS Collaboration, "Observation of a new particle in the search for the Standard Model Higgs boson with the ATLAS detector at the LHC", *Phys. Lett. B* **716** (2012) 1, doi:10.1016/j.physletb.2012.08.020, arXiv:1207.7214.

[2] CMS Collaboration, "Observation of a new boson at a mass of 125 GeV with the CMS experiment at the LHC", *Phys. Lett. B* **716** (2012) 30, doi:10.1016/j.physletb.2012.08.021, arXiv:1207.7235.

[3] CMS Collaboration, "Observation of a new boson with mass near 125 GeV in pp collisions at $\sqrt{s} = 7$ and 8 TeV", *JHEP* **06** (2013) 081, doi:10.1007/JHEP06(2013)081, arXiv:1303.4571.

[4] CMS Collaboration, "Precise determination of the mass of the Higgs boson and tests of compatibility of its couplings with the standard model predictions using proton collisions at 7 and 8 TeV", *Eur. Phys. J. C* **75** (2015), no. 5, 212, doi:10.1140/epjc/s10052-015-3351-7, arXiv:1412.8662.

[5] CMS Collaboration, "Constraints on the spin-parity and anomalous HVV couplings of the Higgs boson in proton collisions at 7 and 8 TeV", *Phys. Rev.* **D92** (2015), no. 1, 012004, doi:10.1103/PhysRevD.92.012004, arXiv:1411.3441.

[6] LHC Higgs Cross Section Working Group, S. Dittmaier et al., "Handbook of LHC Higgs Cross Sections: 1. Inclusive Observables", CERN Report CERN-2011-002, 2011. doi:10.5170/CERN-2011-002, arXiv:1101.0593.

[7] D. Ghosh et al., "Looking for an invisible Higgs signal at the LHC", *Phys. Lett. B* **725** (2012) 344, doi:10.1016/j.physletb.2013.07.042, arXiv:1211.7015.

[8] S. P. Martin and J. D. Wells, "Motivation and detectability of an invisibly decaying Higgs boson at the Fermilab Tevatron", *Phys. Rev. D* **60** (1999) 035006, doi:10.1103/PhysRevD.60.035006, arXiv:hep-ph/9903259.

[9] Y. Bai, P. Draper, and J. Shelton, "Measuring the invisible Higgs width at the 7 and 8 TeV LHC", *JHEP* **07** (2012) 192, doi:10.1007/JHEP07(2012)192, arXiv:1112.4496.

[10] D. Curtin *et. al.*, "Exotic decays of the 125 GeV Higgs boson", *Phys. Rev. D* **90** (2014) 075004, `doi:10.1103/PhysRevD.90.075004`, `arXiv:1312.4992`.

[11] A. Djouadi and M. Drees, "Higgs boson decays into light gravitinos", *Phys. Lett. B* **407** (1997) 243, `doi:10.1016/S0370-2693(97)00670-9`.

[12] C. Petersson, A. Romagnoni, and R. Torre, "Higgs decay with monophoton + $\not{E}_T$ signature from low scale supersymmetry breaking", *JHEP* **10** (2012) 016, `doi:10.1007/JHEP10(2012)016`, `arXiv:1203.4563`.

[13] CMS Collaboration, "Search for a Higgs boson decaying into a Z and a photon in pp collisions at $\sqrt{s} = 7$ and 8 TeV", *Phys. Lett. B* **726** (2013) 587, `doi:10.1016/j.physletb.2013.09.057`.

[14] ATLAS Collaboration, "Search for Higgs boson decays to a photon and a Z boson in pp collisions at $\sqrt{s} = 7$ and 8 TeV with the ATLAS detector", *Phys. Lett. B* **732** (2014) 8, `doi:10.1016/j.physletb.2014.03.015`, `arXiv:1402.3051`.

[15] CMS Collaboration, "The CMS experiment at the CERN LHC", *JINST* **3** (2008) S08004, `doi:10.1088/1748-0221/3/08/S08004`.

[16] CMS Collaboration, "Particle–Flow Event Reconstruction in CMS and Performance for Jets, Taus, and $E_{\mathrm{T}}^{\mathrm{miss}}$", CMS Physics Analysis Summary CMS-PAS-PFT-09-001, 2009.

[17] CMS Collaboration, "Commissioning of the particle-flow event reconstruction with the first LHC collisions recorded in the CMS detector", CMS Physics Analysis Summary CMS-PAS-PFT-10-001, 2010.

[18] M. Cacciari and G. P. Salam and G. Soyez, "The anti-k_t jet clustering algorithm", *JHEP* **04** (2008) 063, `doi:10.1088/1126-6708/2008/04/063`, `arXiv:0802.1189`.

[19] M. Cacciari, G. P. Salam, and G. Soyez, "FastJet user manual", *Eur. Phys. J. C* **72** (2012) 1896, `doi:10.1140/epjc/s10052-012-1896-2`, `arXiv:hep-ph/1111.6097`.

[20] M. Cacciari and G. P. Salam, "Dispelling the N^3 myth for the k_t jet-finder", *Phys. Lett. B* **641** (2006) 57, `doi:10.1016/j.physletb.2006.08.037`, `arXiv:hep-ph/0512210`.

[21] CMS Collaboration, "Pileup Jet Identification", CMS Physics Analysis Summary CMS-PAS-JME-13-005, 2013.

[22] J. Alwall et al., "MadGraph/MadEvent v4: the new web generation", *JHEP* **09** (2007) 028, `doi:10.1088/1126-6708/2007/09/028`.

[23] T. Binoth, M. Ciccolini, N. Kauer, and M. Krämer, "Gluon-induced W-boson pair production at the LHC", *JHEP* **12** (2006) 046, `doi:10.1088/1126-6708/2006/12/046`.

[24] T. Sjöstrand, S. Mrenna, and P. Skands, "PYTHIA 6.4 physics and manual", *JHEP* **05** (2006) 026, `doi:10.1088/1126-6708/2006/05/026`.

[25] H.-L. Lai et al., "Uncertainty induced by QCD coupling in the CTEQ global analysis of parton distributions", *Phys. Rev. D* **82** (2010) 054021, `doi:10.1103/PhysRevD.82.054021`, `arXiv:1004.4624`.

[26] H.-L. Lai et al., "New parton distributions for collider physics", *Phys. Rev. D* **82** (2010) 074024, `doi:10.1103/PhysRevD.82.074024`, `arXiv:1007.2241`.

[27] GEANT4 Collaboration, "GEANT4—a simulation toolkit", *Nucl. Instrum. Meth. A* **506** (2003) 250, doi:10.1016/S0168-9002(03)01368-8.

[28] CMS Collaboration, "Performance of photon reconstruction and identification with the CMS detector in proton-proton collisions at $\sqrt{s} = 8$ TeV", *JINST* **10** (2015), no. 08, P08010, doi:10.1088/1748-0221/10/08/P08010, arXiv:1502.02702.

[29] CMS Collaboration, "Search for new phenomena in monophoton final states in proton-proton collisions at $\sqrt{s} = 8$ TeV", (2014). arXiv:1410.8812. Submitted to *Phys. Lett. B*.

[30] CMS Collaboration, "Performance of electron reconstruction and selection with the CMS detector in proton-proton collisions at $\sqrt{s} = 8$ TeV", *JINST* **10** (2015), no. 06, P06005, doi:10.1088/1748-0221/10/06/P06005, arXiv:1502.02701.

[31] CMS Collaboration, "Missing transverse energy performance of the CMS detector", *JINST* **6** (2011) P09001, doi:10.1088/1748-0221/6/09/P09001.

[32] CMS Collaboration, "Measurement of Higgs boson production and properties in the WW decay channel with leptonic final states", *JHEP* **01** (2014) 096, doi:10.1007/JHEP01(2014)096.

[33] CMS Collaboration, "Observation of the diphoton decay of the Higgs boson and measurement of its properties", *Eur. Phys. J. C* **74** (2014) 3076, doi:10.1140/epjc/s10052-014-3076-z, arXiv:1407.0558.

[34] CMS Collaboration, "Identification of b-quark jets with the CMS experiment", *J. Instrum.* **8** (2012) P04013, doi:10.1088/1748-0221/8/04/P04013.

[35] CMS Collaboration, "Measurement of the inclusive W and Z production cross sections in pp collisions at $\sqrt{s} = 7$ TeV with the CMS experiment", *JHEP* **10** (2011) 132, doi:10.1007/JHEP10(2011)132.

[36] CMS Collaboration, "Measurements of inclusive W and Z cross sections in pp collisions at $\sqrt{s} = 7$ TeV", *J. High Energy Phys.* **01** (2011) 080, doi:10.1007/JHEP01(2011)080.

[37] CMS Collaboration, "Search for invisible decays of Higgs bosons in the vector boson fusion and associated ZH production modes", *Eur. Phys. J. C* **74** (2014) 2980, doi:10.1140/epjc/s10052-014-2980-6.

[38] CMS Collaboration, "CMS Luminosity Based on Pixel Cluster Counting - Summer 2013 Update", CMS Physics Analysis Summary CMS-PAS-LUM-13-001, 2013.

[39] M. Botje et al., "The PDF4LHC Working Group Interim Recommendations", (2011). arXiv:1101.0538.

[40] S. Alekhin et al., "The PDF4LHC Working Group Interim Report", (2011). arXiv:1101.0536.

[41] A. D. Martin, W. J. Stirling, R. S. Thorne, and G. Watt, "Parton distributions for the LHC", *Eur. Phys. J. C* **63** (2009) 189, doi:10.1140/epjc/s10052-009-1072-5, arXiv:0901.0002.

[42] NNPDF Collaboration, "Impact of heavy quark masses on parton distributions and LHC phenomenology", *Nucl. Phys. B* **849** (2011) doi:10.1016/j.nuclphysb.2011.03.021, arXiv:1101.1300.

[43] J. M. Campbell and R. K. Ellis, “MCFM for the Tevatron and the LHC”, *Nucl. Phys. Proc. Suppl.* (2010) 10, doi:10.1016/j.nuclphysbps.2010.08.011.

[44] ATLAS and CMS Collaborations, LHC Higgs Combination Group, “Procedure for the LHC Higgs boson search combination in Summer 2011”, Technical Report ATL-PHYS-PUB 2011-11, CMS NOTE 2011/005, 2011.

[45] A. L. Read, “Presentation of search results: the CL_s technique”, *J. Phys. G* **28** (2002) 2693, doi:10.1088/0954-3899/28/10/313.

[46] T. Junk, “Confidence level computation for combining searches with small statistics”, *Nucl. Instrum. Meth. A* **434** (1999) 435, doi:10.1016/S0168-9002(99)00498-2.

A The CMS Collaboration

Yerevan Physics Institute, Yerevan, Armenia
V. Khachatryan, A.M. Sirunyan, A. Tumasyan

Institut für Hochenergiephysik der OeAW, Wien, Austria
W. Adam, E. Asilar, T. Bergauer, J. Brandstetter, E. Brondolin, M. Dragicevic, J. Erö, M. Flechl, M. Friedl, R. Frühwirth[1], V.M. Ghete, C. Hartl, N. Hörmann, J. Hrubec, M. Jeitler[1], V. Knünz, A. König, M. Krammer[1], I. Krätschmer, D. Liko, T. Matsushita, I. Mikulec, D. Rabady[2], B. Rahbaran, H. Rohringer, J. Schieck[1], R. Schöfbeck, J. Strauss, W. Treberer-Treberspurg, W. Waltenberger, C.-E. Wulz[1]

National Centre for Particle and High Energy Physics, Minsk, Belarus
V. Mossolov, N. Shumeiko, J. Suarez Gonzalez

Universiteit Antwerpen, Antwerpen, Belgium
S. Alderweireldt, T. Cornelis, E.A. De Wolf, X. Janssen, A. Knutsson, J. Lauwers, S. Luyckx, S. Ochesanu, R. Rougny, M. Van De Klundert, H. Van Haevermaet, P. Van Mechelen, N. Van Remortel, A. Van Spilbeeck

Vrije Universiteit Brussel, Brussel, Belgium
S. Abu Zeid, F. Blekman, J. D'Hondt, N. Daci, I. De Bruyn, K. Deroover, N. Heracleous, J. Keaveney, S. Lowette, L. Moreels, A. Olbrechts, Q. Python, D. Strom, S. Tavernier, W. Van Doninck, P. Van Mulders, G.P. Van Onsem, I. Van Parijs

Université Libre de Bruxelles, Bruxelles, Belgium
P. Barria, C. Caillol, B. Clerbaux, G. De Lentdecker, H. Delannoy, G. Fasanella, L. Favart, A.P.R. Gay, A. Grebenyuk, T. Lenzi, A. Léonard, T. Maerschalk, A. Marinov, L. Perniè, A. Randle-conde, T. Reis, T. Seva, C. Vander Velde, P. Vanlaer, R. Yonamine, F. Zenoni, F. Zhang[3]

Ghent University, Ghent, Belgium
K. Beernaert, L. Benucci, A. Cimmino, S. Crucy, D. Dobur, A. Fagot, G. Garcia, M. Gul, J. Mccartin, A.A. Ocampo Rios, D. Poyraz, D. Ryckbosch, S. Salva, M. Sigamani, N. Strobbe, M. Tytgat, W. Van Driessche, E. Yazgan, N. Zaganidis

Université Catholique de Louvain, Louvain-la-Neuve, Belgium
S. Basegmez, C. Beluffi[4], O. Bondu, S. Brochet, G. Bruno, R. Castello, A. Caudron, L. Ceard, G.G. Da Silveira, C. Delaere, D. Favart, L. Forthomme, A. Giammanco[5], J. Hollar, A. Jafari, P. Jez, M. Komm, V. Lemaitre, A. Mertens, C. Nuttens, L. Perrini, A. Pin, K. Piotrzkowski, A. Popov[6], L. Quertenmont, M. Selvaggi, M. Vidal Marono

Université de Mons, Mons, Belgium
N. Beliy, G.H. Hammad

Centro Brasileiro de Pesquisas Fisicas, Rio de Janeiro, Brazil
W.L. Aldá Júnior, G.A. Alves, L. Brito, M. Correa Martins Junior, C. Hensel, C. Mora Herrera, A. Moraes, M.E. Pol, P. Rebello Teles

Universidade do Estado do Rio de Janeiro, Rio de Janeiro, Brazil
E. Belchior Batista Das Chagas, W. Carvalho, J. Chinellato[7], A. Custódio, E.M. Da Costa, D. De Jesus Damiao, C. De Oliveira Martins, S. Fonseca De Souza, L.M. Huertas Guativa, H. Malbouisson, D. Matos Figueiredo, L. Mundim, H. Nogima, W.L. Prado Da Silva, A. Santoro, A. Sznajder, E.J. Tonelli Manganote[7], A. Vilela Pereira

Universidade Estadual Paulista [a], Universidade Federal do ABC [b], São Paulo, Brazil
S. Ahuja[a], C.A. Bernardes[b], A. De Souza Santos[b], S. Dogra[a], T.R. Fernandez Perez Tomei[a], E.M. Gregores[b], P.G. Mercadante[b], C.S. Moon[a,8], S.F. Novaes[a], Sandra S. Padula[a], D. Romero Abad, J.C. Ruiz Vargas

Institute for Nuclear Research and Nuclear Energy, Sofia, Bulgaria
A. Aleksandrov, V. Genchev[†], R. Hadjiiska, P. Iaydjiev, S. Piperov, M. Rodozov, S. Stoykova, G. Sultanov, M. Vutova

University of Sofia, Sofia, Bulgaria
A. Dimitrov, I. Glushkov, L. Litov, B. Pavlov, P. Petkov

Institute of High Energy Physics, Beijing, China
M. Ahmad, J.G. Bian, G.M. Chen, H.S. Chen, M. Chen, T. Cheng, R. Du, C.H. Jiang, R. Plestina[9], F. Romeo, S.M. Shaheen, J. Tao, C. Wang, Z. Wang, H. Zhang

State Key Laboratory of Nuclear Physics and Technology, Peking University, Beijing, China
C. Asawatangtrakuldee, Y. Ban, Q. Li, S. Liu, Y. Mao, S.J. Qian, D. Wang, Z. Xu, W. Zou

Universidad de Los Andes, Bogota, Colombia
C. Avila, A. Cabrera, L.F. Chaparro Sierra, C. Florez, J.P. Gomez, B. Gomez Moreno, J.C. Sanabria

University of Split, Faculty of Electrical Engineering, Mechanical Engineering and Naval Architecture, Split, Croatia
N. Godinovic, D. Lelas, D. Polic, I. Puljak, P.M. Ribeiro Cipriano

University of Split, Faculty of Science, Split, Croatia
Z. Antunovic, M. Kovac

Institute Rudjer Boskovic, Zagreb, Croatia
V. Brigljevic, K. Kadija, J. Luetic, S. Micanovic, L. Sudic

University of Cyprus, Nicosia, Cyprus
A. Attikis, G. Mavromanolakis, J. Mousa, C. Nicolaou, F. Ptochos, P.A. Razis, H. Rykaczewski

Charles University, Prague, Czech Republic
M. Bodlak, M. Finger[10], M. Finger Jr.[10]

Academy of Scientific Research and Technology of the Arab Republic of Egypt, Egyptian Network of High Energy Physics, Cairo, Egypt
A.A. Abdelalim[11], A. Awad, A. Mahrous[12], A. Radi[13,14]

National Institute of Chemical Physics and Biophysics, Tallinn, Estonia
B. Calpas, M. Kadastik, M. Murumaa, M. Raidal, A. Tiko, C. Veelken

Department of Physics, University of Helsinki, Helsinki, Finland
P. Eerola, J. Pekkanen, M. Voutilainen

Helsinki Institute of Physics, Helsinki, Finland
J. Härkönen, V. Karimäki, R. Kinnunen, T. Lampén, K. Lassila-Perini, S. Lehti, T. Lindén, P. Luukka, T. Mäenpää, T. Peltola, E. Tuominen, J. Tuominiemi, E. Tuovinen, L. Wendland

Lappeenranta University of Technology, Lappeenranta, Finland
J. Talvitie, T. Tuuva

DSM/IRFU, CEA/Saclay, Gif-sur-Yvette, France
M. Besancon, F. Couderc, M. Dejardin, D. Denegri, B. Fabbro, J.L. Faure, C. Favaro, F. Ferri, S. Ganjour, A. Givernaud, P. Gras, G. Hamel de Monchenault, P. Jarry, E. Locci, M. Machet, J. Malcles, J. Rander, A. Rosowsky, M. Titov, A. Zghiche

Laboratoire Leprince-Ringuet, Ecole Polytechnique, IN2P3-CNRS, Palaiseau, France
I. Antropov, S. Baffioni, F. Beaudette, P. Busson, L. Cadamuro, E. Chapon, C. Charlot, T. Dahms, O. Davignon, N. Filipovic, A. Florent, R. Granier de Cassagnac, S. Lisniak, L. Mastrolorenzo, P. Miné, I.N. Naranjo, M. Nguyen, C. Ochando, G. Ortona, P. Paganini, S. Regnard, R. Salerno, J.B. Sauvan, Y. Sirois, T. Strebler, Y. Yilmaz, A. Zabi

Institut Pluridisciplinaire Hubert Curien, Université de Strasbourg, Université de Haute Alsace Mulhouse, CNRS/IN2P3, Strasbourg, France
J.-L. Agram[15], J. Andrea, A. Aubin, D. Bloch, J.-M. Brom, M. Buttignol, E.C. Chabert, N. Chanon, C. Collard, E. Conte[15], X. Coubez, J.-C. Fontaine[15], D. Gelé, U. Goerlach, C. Goetzmann, A.-C. Le Bihan, J.A. Merlin[2], K. Skovpen, P. Van Hove

Centre de Calcul de l'Institut National de Physique Nucleaire et de Physique des Particules, CNRS/IN2P3, Villeurbanne, France
S. Gadrat

Université de Lyon, Université Claude Bernard Lyon 1, CNRS-IN2P3, Institut de Physique Nucléaire de Lyon, Villeurbanne, France
S. Beauceron, C. Bernet, G. Boudoul, E. Bouvier, C.A. Carrillo Montoya, J. Chasserat, R. Chierici, D. Contardo, B. Courbon, P. Depasse, H. El Mamouni, J. Fan, J. Fay, S. Gascon, M. Gouzevitch, B. Ille, F. Lagarde, I.B. Laktineh, M. Lethuillier, L. Mirabito, A.L. Pequegnot, S. Perries, J.D. Ruiz Alvarez, D. Sabes, L. Sgandurra, V. Sordini, M. Vander Donckt, P. Verdier, S. Viret, H. Xiao

Georgian Technical University, Tbilisi, Georgia
T. Toriashvili[16]

Tbilisi State University, Tbilisi, Georgia
Z. Tsamalaidze[10]

RWTH Aachen University, I. Physikalisches Institut, Aachen, Germany
C. Autermann, S. Beranek, M. Edelhoff, L. Feld, A. Heister, M.K. Kiesel, K. Klein, M. Lipinski, A. Ostapchuk, M. Preuten, F. Raupach, S. Schael, J.F. Schulte, T. Verlage, H. Weber, B. Wittmer, V. Zhukov[6]

RWTH Aachen University, III. Physikalisches Institut A, Aachen, Germany
M. Ata, M. Brodski, E. Dietz-Laursonn, D. Duchardt, M. Endres, M. Erdmann, S. Erdweg, T. Esch, R. Fischer, A. Güth, T. Hebbeker, C. Heidemann, K. Hoepfner, D. Klingebiel, S. Knutzen, P. Kreuzer, M. Merschmeyer, A. Meyer, P. Millet, M. Olschewski, K. Padeken, P. Papacz, T. Pook, M. Radziej, H. Reithler, M. Rieger, F. Scheuch, L. Sonnenschein, D. Teyssier, S. Thüer

RWTH Aachen University, III. Physikalisches Institut B, Aachen, Germany
V. Cherepanov, Y. Erdogan, G. Flügge, H. Geenen, M. Geisler, F. Hoehle, B. Kargoll, T. Kress, Y. Kuessel, A. Künsken, J. Lingemann[2], A. Nehrkorn, A. Nowack, I.M. Nugent, C. Pistone, O. Pooth, A. Stahl

Deutsches Elektronen-Synchrotron, Hamburg, Germany
M. Aldaya Martin, I. Asin, N. Bartosik, O. Behnke, U. Behrens, A.J. Bell, K. Borras, A. Burgmeier, A. Cakir, L. Calligaris, A. Campbell, S. Choudhury, F. Costanza, C. Diez

Pardos, G. Dolinska, S. Dooling, T. Dorland, G. Eckerlin, D. Eckstein, T. Eichhorn, G. Flucke, E. Gallo, J. Garay Garcia, A. Geiser, A. Gizhko, P. Gunnellini, J. Hauk, M. Hempel[17], H. Jung, A. Kalogeropoulos, O. Karacheban[17], M. Kasemann, P. Katsas, J. Kieseler, C. Kleinwort, I. Korol, W. Lange, J. Leonard, K. Lipka, A. Lobanov, W. Lohmann[17], R. Mankel, I. Marfin[17], I.-A. Melzer-Pellmann, A.B. Meyer, G. Mittag, J. Mnich, A. Mussgiller, S. Naumann-Emme, A. Nayak, E. Ntomari, H. Perrey, D. Pitzl, R. Placakyte, A. Raspereza, B. Roland, M.Ö. Sahin, P. Saxena, T. Schoerner-Sadenius, M. Schröder, C. Seitz, S. Spannagel, K.D. Trippkewitz, C. Wissing

University of Hamburg, Hamburg, Germany
V. Blobel, M. Centis Vignali, A.R. Draeger, J. Erfle, E. Garutti, K. Goebel, D. Gonzalez, M. Görner, J. Haller, M. Hoffmann, R.S. Höing, A. Junkes, R. Klanner, R. Kogler, T. Lapsien, T. Lenz, I. Marchesini, D. Marconi, D. Nowatschin, J. Ott, F. Pantaleo[2], T. Peiffer, A. Perieanu, N. Pietsch, J. Poehlsen, D. Rathjens, C. Sander, H. Schettler, P. Schleper, E. Schlieckau, A. Schmidt, J. Schwandt, M. Seidel, V. Sola, H. Stadie, G. Steinbrück, H. Tholen, D. Troendle, E. Usai, L. Vanelderen, A. Vanhoefer

Institut für Experimentelle Kernphysik, Karlsruhe, Germany
M. Akbiyik, C. Barth, C. Baus, J. Berger, C. Böser, E. Butz, T. Chwalek, F. Colombo, W. De Boer, A. Descroix, A. Dierlamm, S. Fink, F. Frensch, M. Giffels, A. Gilbert, F. Hartmann[2], S.M. Heindl, U. Husemann, F. Kassel[2], I. Katkov[6], A. Kornmayer[2], P. Lobelle Pardo, B. Maier, H. Mildner, M.U. Mozer, T. Müller, Th. Müller, M. Plagge, G. Quast, K. Rabbertz, S. Röcker, F. Roscher, H.J. Simonis, F.M. Stober, R. Ulrich, J. Wagner-Kuhr, S. Wayand, M. Weber, T. Weiler, C. Wöhrmann, R. Wolf

Institute of Nuclear and Particle Physics (INPP), NCSR Demokritos, Aghia Paraskevi, Greece
G. Anagnostou, G. Daskalakis, T. Geralis, V.A. Giakoumopoulou, A. Kyriakis, D. Loukas, A. Psallidas, I. Topsis-Giotis

University of Athens, Athens, Greece
A. Agapitos, S. Kesisoglou, A. Panagiotou, N. Saoulidou, E. Tziaferi

University of Ioánnina, Ioánnina, Greece
I. Evangelou, G. Flouris, C. Foudas, P. Kokkas, N. Loukas, N. Manthos, I. Papadopoulos, E. Paradas, J. Strologas

Wigner Research Centre for Physics, Budapest, Hungary
G. Bencze, C. Hajdu, A. Hazi, P. Hidas, D. Horvath[18], F. Sikler, V. Veszpremi, G. Vesztergombi[19], A.J. Zsigmond

Institute of Nuclear Research ATOMKI, Debrecen, Hungary
N. Beni, S. Czellar, J. Karancsi[20], J. Molnar, Z. Szillasi

University of Debrecen, Debrecen, Hungary
M. Bartók[21], A. Makovec, P. Raics, Z.L. Trocsanyi, B. Ujvari

National Institute of Science Education and Research, Bhubaneswar, India
P. Mal, K. Mandal, N. Sahoo, S.K. Swain

Panjab University, Chandigarh, India
S. Bansal, S.B. Beri, V. Bhatnagar, R. Chawla, R. Gupta, U.Bhawandeep, A.K. Kalsi, A. Kaur, M. Kaur, R. Kumar, A. Mehta, M. Mittal, J.B. Singh, G. Walia

University of Delhi, Delhi, India
Ashok Kumar, Arun Kumar, A. Bhardwaj, B.C. Choudhary, R.B. Garg, A. Kumar, S. Malhotra, M. Naimuddin, N. Nishu, K. Ranjan, R. Sharma, V. Sharma

Saha Institute of Nuclear Physics, Kolkata, India
S. Banerjee, S. Bhattacharya, K. Chatterjee, S. Dey, S. Dutta, Sa. Jain, N. Majumdar, A. Modak, K. Mondal, S. Mukherjee, S. Mukhopadhyay, A. Roy, D. Roy, S. Roy Chowdhury, S. Sarkar, M. Sharan

Bhabha Atomic Research Centre, Mumbai, India
A. Abdulsalam, R. Chudasama, D. Dutta, V. Jha, V. Kumar, A.K. Mohanty[2], L.M. Pant, P. Shukla, A. Topkar

Tata Institute of Fundamental Research, Mumbai, India
T. Aziz, S. Banerjee, S. Bhowmik[22], R.M. Chatterjee, R.K. Dewanjee, S. Dugad, S. Ganguly, S. Ghosh, M. Guchait, A. Gurtu[23], G. Kole, S. Kumar, B. Mahakud, M. Maity[22], G. Majumder, K. Mazumdar, S. Mitra, G.B. Mohanty, B. Parida, T. Sarkar[22], K. Sudhakar, N. Sur, B. Sutar, N. Wickramage[24]

Indian Institute of Science Education and Research (IISER), Pune, India
S. Chauhan, S. Dube, S. Sharma

Institute for Research in Fundamental Sciences (IPM), Tehran, Iran
H. Bakhshiansohi, H. Behnamian, S.M. Etesami[25], A. Fahim[26], R. Goldouzian, M. Khakzad, M. Mohammadi Najafabadi, M. Naseri, S. Paktinat Mehdiabadi, F. Rezaei Hosseinabadi, B. Safarzadeh[27], M. Zeinali

University College Dublin, Dublin, Ireland
M. Felcini, M. Grunewald

INFN Sezione di Bari [a], Università di Bari [b], Politecnico di Bari [c], Bari, Italy
M. Abbrescia[a,b], C. Calabria[a,b], C. Caputo[a,b], S.S. Chhibra[a,b], A. Colaleo[a], D. Creanza[a,c], L. Cristella[a,b], N. De Filippis[a,c], M. De Palma[a,b], L. Fiore[a], G. Iaselli[a,c], G. Maggi[a,c], M. Maggi[a], G. Miniello[a,b], S. My[a,c], S. Nuzzo[a,b], A. Pompili[a,b], G. Pugliese[a,c], R. Radogna[a,b], A. Ranieri[a], G. Selvaggi[a,b], L. Silvestris[a,2], R. Venditti[a,b], P. Verwilligen[a]

INFN Sezione di Bologna [a], Università di Bologna [b], Bologna, Italy
G. Abbiendi[a], C. Battilana[2], A.C. Benvenuti[a], D. Bonacorsi[a,b], S. Braibant-Giacomelli[a,b], L. Brigliadori[a,b], R. Campanini[a,b], P. Capiluppi[a,b], A. Castro[a,b], F.R. Cavallo[a], G. Codispoti[a,b], M. Cuffiani[a,b], G.M. Dallavalle[a], F. Fabbri[a], A. Fanfani[a,b], D. Fasanella[a,b], P. Giacomelli[a], C. Grandi[a], L. Guiducci[a,b], S. Marcellini[a], G. Masetti[a], A. Montanari[a], F.L. Navarria[a,b], A. Perrotta[a], A.M. Rossi[a,b], T. Rovelli[a,b], G.P. Siroli[a,b], N. Tosi[a,b], R. Travaglini[a,b]

INFN Sezione di Catania [a], Università di Catania [b], CSFNSM [c], Catania, Italy
G. Cappello[a], M. Chiorboli[a,b], S. Costa[a,b], F. Giordano[a], R. Potenza[a,b], A. Tricomi[a,b], C. Tuve[a,b]

INFN Sezione di Firenze [a], Università di Firenze [b], Firenze, Italy
G. Barbagli[a], V. Ciulli[a,b], C. Civinini[a], R. D'Alessandro[a,b], E. Focardi[a,b], S. Gonzi[a,b], V. Gori[a,b], P. Lenzi[a,b], M. Meschini[a], S. Paoletti[a], G. Sguazzoni[a], A. Tropiano[a,b], L. Viliani[a,b]

INFN Laboratori Nazionali di Frascati, Frascati, Italy
L. Benussi, S. Bianco, F. Fabbri, D. Piccolo

INFN Sezione di Genova [a], Università di Genova [b], Genova, Italy
V. Calvelli[a,b], F. Ferro[a], M. Lo Vetere[a,b], M.R. Monge[a,b], E. Robutti[a], S. Tosi[a,b]

INFN Sezione di Milano-Bicocca [a], Università di Milano-Bicocca [b], Milano, Italy
L. Brianza, M.E. Dinardo[a,b], S. Fiorendi[a,b], S. Gennai[a], R. Gerosa[a,b], A. Ghezzi[a,b], P. Govoni[a,b], S. Malvezzi[a], R.A. Manzoni[a,b], B. Marzocchi[a,b,2], D. Menasce[a], L. Moroni[a], M. Paganoni[a,b], D. Pedrini[a], S. Ragazzi[a,b], N. Redaelli[a], T. Tabarelli de Fatis[a,b]

INFN Sezione di Napoli [a], Università di Napoli 'Federico II' [b], Napoli, Italy, Università della Basilicata [c], Potenza, Italy, Università G. Marconi [d], Roma, Italy
S. Buontempo[a], N. Cavallo[a,c], S. Di Guida[a,d,2], M. Esposito[a,b], F. Fabozzi[a,c], A.O.M. Iorio[a,b], G. Lanza[a], L. Lista[a], S. Meola[a,d,2], M. Merola[a], P. Paolucci[a,2], C. Sciacca[a,b], F. Thyssen

INFN Sezione di Padova [a], Università di Padova [b], Padova, Italy, Università di Trento [c], Trento, Italy
P. Azzi[a,2], N. Bacchetta[a], L. Benato[a,b], D. Bisello[a,b], A. Boletti[a,b], R. Carlin[a,b], P. Checchia[a], M. Dall'Osso[a,b,2], T. Dorigo[a], F. Gasparini[a,b], U. Gasparini[a,b], A. Gozzelino[a], S. Lacaprara[a], M. Margoni[a,b], A.T. Meneguzzo[a,b], F. Montecassiano[a], M. Passaseo[a], J. Pazzini[a,b], M. Pegoraro[a], N. Pozzobon[a,b], P. Ronchese[a,b], F. Simonetto[a,b], E. Torassa[a], M. Tosi[a,b], S. Vanini[a,b], S. Ventura[a], M. Zanetti, P. Zotto[a,b], A. Zucchetta[a,b,2]

INFN Sezione di Pavia [a], Università di Pavia [b], Pavia, Italy
A. Braghieri[a], A. Magnani[a], P. Montagna[a,b], S.P. Ratti[a,b], V. Re[a], C. Riccardi[a,b], P. Salvini[a], I. Vai[a], P. Vitulo[a,b]

INFN Sezione di Perugia [a], Università di Perugia [b], Perugia, Italy
L. Alunni Solestizi[a,b], M. Biasini[a,b], G.M. Bilei[a], D. Ciangottini[a,b,2], L. Fanò[a,b], P. Lariccia[a,b], G. Mantovani[a,b], M. Menichelli[a], A. Saha[a], A. Santocchia[a,b], A. Spiezia[a,b]

INFN Sezione di Pisa [a], Università di Pisa [b], Scuola Normale Superiore di Pisa [c], Pisa, Italy
K. Androsov[a,28], P. Azzurri[a], G. Bagliesi[a], J. Bernardini[a], T. Boccali[a], G. Broccolo[a,c], R. Castaldi[a], M.A. Ciocci[a,28], R. Dell'Orso[a], S. Donato[a,c,2], G. Fedi, L. Foà[a,c†], A. Giassi[a], M.T. Grippo[a,28], F. Ligabue[a,c], T. Lomtadze[a], L. Martini[a,b], A. Messineo[a,b], F. Palla[a], A. Rizzi[a,b], A. Savoy-Navarro[a,29], A.T. Serban[a], P. Spagnolo[a], P. Squillacioti[a,28], R. Tenchini[a], G. Tonelli[a,b], A. Venturi[a], P.G. Verdini[a]

INFN Sezione di Roma [a], Università di Roma [b], Roma, Italy
L. Barone[a,b], F. Cavallari[a], G. D'imperio[a,b,2], D. Del Re[a,b], M. Diemoz[a], S. Gelli[a,b], C. Jorda[a], E. Longo[a,b], F. Margaroli[a,b], P. Meridiani[a], F. Micheli[a,b], G. Organtini[a,b], R. Paramatti[a], F. Preiato[a,b], S. Rahatlou[a,b], C. Rovelli[a], F. Santanastasio[a,b], P. Traczyk[a,b,2]

INFN Sezione di Torino [a], Università di Torino [b], Torino, Italy, Università del Piemonte Orientale [c], Novara, Italy
N. Amapane[a,b], R. Arcidiacono[a,c,2], S. Argiro[a,b], M. Arneodo[a,c], R. Bellan[a,b], C. Biino[a], N. Cartiglia[a], M. Costa[a,b], R. Covarelli[a,b], A. Degano[a,b], N. Demaria[a], L. Finco[a,b,2], B. Kiani[a,b], C. Mariotti[a], S. Maselli[a], E. Migliore[a,b], V. Monaco[a,b], E. Monteil[a,b], M. Musich[a], M.M. Obertino[a,b], L. Pacher[a,b], N. Pastrone[a], M. Pelliccioni[a], G.L. Pinna Angioni[a,b], F. Ravera[a,b], A. Romero[a,b], M. Ruspa[a,c], R. Sacchi[a,b], A. Solano[a,b], A. Staiano[a], U. Tamponi[a]

INFN Sezione di Trieste [a], Università di Trieste [b], Trieste, Italy
S. Belforte[a], V. Candelise[a,b,2], M. Casarsa[a], F. Cossutti[a], G. Della Ricca[a,b], B. Gobbo[a], C. La Licata[a,b], M. Marone[a,b], A. Schizzi[a,b], T. Umer[a,b], A. Zanetti[a]

Kangwon National University, Chunchon, Korea
S. Chang, A. Kropivnitskaya, S.K. Nam

Kyungpook National University, Daegu, Korea
D.H. Kim, G.N. Kim, M.S. Kim, D.J. Kong, S. Lee, Y.D. Oh, A. Sakharov, D.C. Son

Chonbuk National University, Jeonju, Korea
J.A. Brochero Cifuentes, H. Kim, T.J. Kim, M.S. Ryu

Chonnam National University, Institute for Universe and Elementary Particles, Kwangju, Korea
S. Song

Korea University, Seoul, Korea
S. Choi, Y. Go, D. Gyun, B. Hong, M. Jo, H. Kim, Y. Kim, B. Lee, K. Lee, K.S. Lee, S. Lee, S.K. Park, Y. Roh

Seoul National University, Seoul, Korea
H.D. Yoo

University of Seoul, Seoul, Korea
M. Choi, H. Kim, J.H. Kim, J.S.H. Lee, I.C. Park, G. Ryu

Sungkyunkwan University, Suwon, Korea
Y. Choi, Y.K. Choi, J. Goh, D. Kim, E. Kwon, J. Lee, I. Yu

Vilnius University, Vilnius, Lithuania
A. Juodagalvis, J. Vaitkus

National Centre for Particle Physics, Universiti Malaya, Kuala Lumpur, Malaysia
I. Ahmed, Z.A. Ibrahim, J.R. Komaragiri, M.A.B. Md Ali[30], F. Mohamad Idris[31], W.A.T. Wan Abdullah, M.N. Yusli

Centro de Investigacion y de Estudios Avanzados del IPN, Mexico City, Mexico
E. Casimiro Linares, H. Castilla-Valdez, E. De La Cruz-Burelo, I. Heredia-de La Cruz[32], A. Hernandez-Almada, R. Lopez-Fernandez, A. Sanchez-Hernandez

Universidad Iberoamericana, Mexico City, Mexico
S. Carrillo Moreno, F. Vazquez Valencia

Benemerita Universidad Autonoma de Puebla, Puebla, Mexico
S. Carpinteyro, I. Pedraza, H.A. Salazar Ibarguen

Universidad Autónoma de San Luis Potosí, San Luis Potosí, Mexico
A. Morelos Pineda

University of Auckland, Auckland, New Zealand
D. Krofcheck

University of Canterbury, Christchurch, New Zealand
P.H. Butler, S. Reucroft

National Centre for Physics, Quaid-I-Azam University, Islamabad, Pakistan
A. Ahmad, M. Ahmad, Q. Hassan, H.R. Hoorani, W.A. Khan, T. Khurshid, M. Shoaib

National Centre for Nuclear Research, Swierk, Poland
H. Bialkowska, M. Bluj, B. Boimska, T. Frueboes, M. Górski, M. Kazana, K. Nawrocki, K. Romanowska-Rybinska, M. Szleper, P. Zalewski

Institute of Experimental Physics, Faculty of Physics, University of Warsaw, Warsaw, Poland
G. Brona, K. Bunkowski, K. Doroba, A. Kalinowski, M. Konecki, J. Krolikowski, M. Misiura, M. Olszewski, M. Walczak

Laboratório de Instrumentação e Física Experimental de Partículas, Lisboa, Portugal
P. Bargassa, C. Beirão Da Cruz E Silva, A. Di Francesco, P. Faccioli, P.G. Ferreira Parracho, M. Gallinaro, N. Leonardo, L. Lloret Iglesias, F. Nguyen, J. Rodrigues Antunes, J. Seixas, O. Toldaiev, D. Vadruccio, J. Varela, P. Vischia

Joint Institute for Nuclear Research, Dubna, Russia
S. Afanasiev, P. Bunin, M. Gavrilenko, I. Golutvin, I. Gorbunov, A. Kamenev, V. Karjavin, V. Konoplyanikov, A. Lanev, A. Malakhov, V. Matveev[33], P. Moisenz, V. Palichik, V. Perelygin, S. Shmatov, S. Shulha, N. Skatchkov, V. Smirnov, A. Zarubin

Petersburg Nuclear Physics Institute, Gatchina (St. Petersburg), Russia
V. Golovtsov, Y. Ivanov, V. Kim[34], E. Kuznetsova, P. Levchenko, V. Murzin, V. Oreshkin, I. Smirnov, V. Sulimov, L. Uvarov, S. Vavilov, A. Vorobyev

Institute for Nuclear Research, Moscow, Russia
Yu. Andreev, A. Dermenev, S. Gninenko, N. Golubev, A. Karneyeu, M. Kirsanov, N. Krasnikov, A. Pashenkov, D. Tlisov, A. Toropin

Institute for Theoretical and Experimental Physics, Moscow, Russia
V. Epshteyn, V. Gavrilov, N. Lychkovskaya, V. Popov, I. Pozdnyakov, G. Safronov, A. Spiridonov, E. Vlasov, A. Zhokin

National Research Nuclear University 'Moscow Engineering Physics Institute' (MEPhI), Moscow, Russia
A. Bylinkin

P.N. Lebedev Physical Institute, Moscow, Russia
V. Andreev, M. Azarkin[35], I. Dremin[35], M. Kirakosyan, A. Leonidov[35], G. Mesyats, S.V. Rusakov, A. Vinogradov

Skobeltsyn Institute of Nuclear Physics, Lomonosov Moscow State University, Moscow, Russia
A. Baskakov, A. Belyaev, E. Boos, V. Bunichev, M. Dubinin[36], L. Dudko, A. Ershov, V. Klyukhin, O. Kodolova, I. Lokhtin, I. Myagkov, S. Obraztsov, S. Petrushanko, V. Savrin, A. Snigirev

State Research Center of Russian Federation, Institute for High Energy Physics, Protvino, Russia
I. Azhgirey, I. Bayshev, S. Bitioukov, V. Kachanov, A. Kalinin, D. Konstantinov, V. Krychkine, V. Petrov, R. Ryutin, A. Sobol, L. Tourtchanovitch, S. Troshin, N. Tyurin, A. Uzunian, A. Volkov

University of Belgrade, Faculty of Physics and Vinca Institute of Nuclear Sciences, Belgrade, Serbia
P. Adzic[37], M. Ekmedzic, J. Milosevic, V. Rekovic

Centro de Investigaciones Energéticas Medioambientales y Tecnológicas (CIEMAT), Madrid, Spain
J. Alcaraz Maestre, E. Calvo, M. Cerrada, M. Chamizo Llatas, N. Colino, B. De La Cruz, A. Delgado Peris, D. Domínguez Vázquez, A. Escalante Del Valle, C. Fernandez Bedoya, J.P. Fernández Ramos, J. Flix, M.C. Fouz, P. Garcia-Abia, O. Gonzalez Lopez, S. Goy Lopez, J.M. Hernandez, M.I. Josa, E. Navarro De Martino, A. Pérez-Calero Yzquierdo, J. Puerta Pelayo, A. Quintario Olmeda, I. Redondo, L. Romero, M.S. Soares

Universidad Autónoma de Madrid, Madrid, Spain
C. Albajar, J.F. de Trocóniz, M. Missiroli, D. Moran

Universidad de Oviedo, Oviedo, Spain
H. Brun, J. Cuevas, J. Fernandez Menendez, S. Folgueras, I. Gonzalez Caballero, E. Palencia Cortezon, J.M. Vizan Garcia

Instituto de Física de Cantabria (IFCA), CSIC-Universidad de Cantabria, Santander, Spain
I.J. Cabrillo, A. Calderon, J.R. Castiñeiras De Saa, P. De Castro Manzano, J. Duarte Campderros, M. Fernandez, G. Gomez, A. Graziano, A. Lopez Virto, J. Marco, R. Marco, C. Martinez Rivero, F. Matorras, F.J. Munoz Sanchez, J. Piedra Gomez, T. Rodrigo, A.Y. Rodríguez-Marrero, A. Ruiz-Jimeno, L. Scodellaro, I. Vila, R. Vilar Cortabitarte

CERN, European Organization for Nuclear Research, Geneva, Switzerland
D. Abbaneo, E. Auffray, G. Auzinger, M. Bachtis, P. Baillon, A.H. Ball, D. Barney, A. Benaglia, J. Bendavid, L. Benhabib, J.F. Benitez, G.M. Berruti, P. Bloch, A. Bocci, A. Bonato, C. Botta, H. Breuker, T. Camporesi, G. Cerminara, S. Colafranceschi[38], M. D'Alfonso, D. d'Enterria, A. Dabrowski, V. Daponte, A. David, M. De Gruttola, F. De Guio, A. De Roeck, S. De Visscher, E. Di Marco, M. Dobson, M. Dordevic, T. du Pree, N. Dupont, A. Elliott-Peisert, G. Franzoni, W. Funk, D. Gigi, K. Gill, D. Giordano, M. Girone, F. Glege, R. Guida, S. Gundacker, M. Guthoff, J. Hammer, M. Hansen, P. Harris, J. Hegeman, V. Innocente, P. Janot, H. Kirschenmann, M.J. Kortelainen, K. Kousouris, K. Krajczar, P. Lecoq, C. Lourenço, M.T. Lucchini, N. Magini, L. Malgeri, M. Mannelli, A. Martelli, L. Masetti, F. Meijers, S. Mersi, E. Meschi, F. Moortgat, S. Morovic, M. Mulders, M.V. Nemallapudi, H. Neugebauer, S. Orfanelli[39], L. Orsini, L. Pape, E. Perez, A. Petrilli, G. Petrucciani, A. Pfeiffer, D. Piparo, A. Racz, G. Rolandi[40], M. Rovere, M. Ruan, H. Sakulin, C. Schäfer, C. Schwick, A. Sharma, P. Silva, M. Simon, P. Sphicas[41], D. Spiga, J. Steggemann, B. Stieger, M. Stoye, Y. Takahashi, D. Treille, A. Triossi, A. Tsirou, G.I. Veres[19], N. Wardle, H.K. Wöhri, A. Zagozdzinska[42], W.D. Zeuner

Paul Scherrer Institut, Villigen, Switzerland
W. Bertl, K. Deiters, W. Erdmann, R. Horisberger, Q. Ingram, H.C. Kaestli, D. Kotlinski, U. Langenegger, D. Renker, T. Rohe

Institute for Particle Physics, ETH Zurich, Zurich, Switzerland
F. Bachmair, L. Bäni, L. Bianchini, M.A. Buchmann, B. Casal, G. Dissertori, M. Dittmar, M. Donegà, M. Dünser, P. Eller, C. Grab, C. Heidegger, D. Hits, J. Hoss, G. Kasieczka, W. Lustermann, B. Mangano, A.C. Marini, M. Marionneau, P. Martinez Ruiz del Arbol, M. Masciovecchio, D. Meister, P. Musella, F. Nessi-Tedaldi, F. Pandolfi, J. Pata, F. Pauss, L. Perrozzi, M. Peruzzi, M. Quittnat, M. Rossini, A. Starodumov[43], M. Takahashi, V.R. Tavolaro, K. Theofilatos, R. Wallny

Universität Zürich, Zurich, Switzerland
T.K. Aarrestad, C. Amsler[44], L. Caminada, M.F. Canelli, V. Chiochia, A. De Cosa, C. Galloni, A. Hinzmann, T. Hreus, B. Kilminster, C. Lange, J. Ngadiuba, D. Pinna, P. Robmann, F.J. Ronga, D. Salerno, Y. Yang

National Central University, Chung-Li, Taiwan
M. Cardaci, K.H. Chen, T.H. Doan, C. Ferro, Sh. Jain, R. Khurana, M. Konyushikhin, C.M. Kuo, W. Lin, Y.J. Lu, R. Volpe, S.S. Yu

National Taiwan University (NTU), Taipei, Taiwan
R. Bartek, P. Chang, Y.H. Chang, Y.W. Chang, Y. Chao, K.F. Chen, P.H. Chen, C. Dietz, F. Fiori,

U. Grundler, W.-S. Hou, Y. Hsiung, Y.F. Liu, R.-S. Lu, M. Miñano Moya, E. Petrakou, J.F. Tsai, Y.M. Tzeng

Chulalongkorn University, Faculty of Science, Department of Physics, Bangkok, Thailand
B. Asavapibhop, K. Kovitanggoon, G. Singh, N. Srimanobhas, N. Suwonjandee

Cukurova University, Adana, Turkey
A. Adiguzel, S. Cerci[45], C. Dozen, S. Girgis, G. Gokbulut, Y. Guler, E. Gurpinar, I. Hos, E.E. Kangal[46], A. Kayis Topaksu, G. Onengut[47], K. Ozdemir[48], S. Ozturk[49], B. Tali[45], H. Topakli[49], M. Vergili, C. Zorbilmez

Middle East Technical University, Physics Department, Ankara, Turkey
I.V. Akin, B. Bilin, S. Bilmis, B. Isildak[50], G. Karapinar[51], U.E. Surat, M. Yalvac, M. Zeyrek

Bogazici University, Istanbul, Turkey
E.A. Albayrak[52], E. Gülmez, M. Kaya[53], O. Kaya[54], T. Yetkin[55]

Istanbul Technical University, Istanbul, Turkey
K. Cankocak, S. Sen[56], F.I. Vardarlı

Institute for Scintillation Materials of National Academy of Science of Ukraine, Kharkov, Ukraine
B. Grynyov

National Scientific Center, Kharkov Institute of Physics and Technology, Kharkov, Ukraine
L. Levchuk, P. Sorokin

University of Bristol, Bristol, United Kingdom
R. Aggleton, F. Ball, L. Beck, J.J. Brooke, E. Clement, D. Cussans, H. Flacher, J. Goldstein, M. Grimes, G.P. Heath, H.F. Heath, J. Jacob, L. Kreczko, C. Lucas, Z. Meng, D.M. Newbold[57], S. Paramesvaran, A. Poll, T. Sakuma, S. Seif El Nasr-storey, S. Senkin, D. Smith, V.J. Smith

Rutherford Appleton Laboratory, Didcot, United Kingdom
K.W. Bell, A. Belyaev[58], C. Brew, R.M. Brown, D.J.A. Cockerill, J.A. Coughlan, K. Harder, S. Harper, E. Olaiya, D. Petyt, C.H. Shepherd-Themistocleous, A. Thea, L. Thomas, I.R. Tomalin, T. Williams, W.J. Womersley, S.D. Worm

Imperial College, London, United Kingdom
M. Baber, R. Bainbridge, O. Buchmuller, A. Bundock, D. Burton, S. Casasso, M. Citron, D. Colling, L. Corpe, N. Cripps, P. Dauncey, G. Davies, A. De Wit, M. Della Negra, P. Dunne, A. Elwood, W. Ferguson, J. Fulcher, D. Futyan, G. Hall, G. Iles, G. Karapostoli, M. Kenzie, R. Lane, R. Lucas[57], L. Lyons, A.-M. Magnan, S. Malik, J. Nash, A. Nikitenko[43], J. Pela, M. Pesaresi, K. Petridis, D.M. Raymond, A. Richards, A. Rose, C. Seez, A. Tapper, K. Uchida, M. Vazquez Acosta[59], T. Virdee, S.C. Zenz

Brunel University, Uxbridge, United Kingdom
J.E. Cole, P.R. Hobson, A. Khan, P. Kyberd, D. Leggat, D. Leslie, I.D. Reid, P. Symonds, L. Teodorescu, M. Turner

Baylor University, Waco, USA
A. Borzou, K. Call, J. Dittmann, K. Hatakeyama, A. Kasmi, H. Liu, N. Pastika

The University of Alabama, Tuscaloosa, USA
O. Charaf, S.I. Cooper, C. Henderson, P. Rumerio

Boston University, Boston, USA
A. Avetisyan, T. Bose, C. Fantasia, D. Gastler, P. Lawson, D. Rankin, C. Richardson, J. Rohlf, J. St. John, L. Sulak, D. Zou

Brown University, Providence, USA
J. Alimena, E. Berry, S. Bhattacharya, D. Cutts, N. Dhingra, A. Ferapontov, A. Garabedian, U. Heintz, E. Laird, G. Landsberg, Z. Mao, M. Narain, S. Sagir, T. Sinthuprasith

University of California, Davis, Davis, USA
R. Breedon, G. Breto, M. Calderon De La Barca Sanchez, S. Chauhan, M. Chertok, J. Conway, R. Conway, P.T. Cox, R. Erbacher, M. Gardner, W. Ko, R. Lander, M. Mulhearn, D. Pellett, J. Pilot, F. Ricci-Tam, S. Shalhout, J. Smith, M. Squires, D. Stolp, M. Tripathi, S. Wilbur, R. Yohay

University of California, Los Angeles, USA
R. Cousins, P. Everaerts, C. Farrell, J. Hauser, M. Ignatenko, D. Saltzberg, E. Takasugi, V. Valuev, M. Weber

University of California, Riverside, Riverside, USA
K. Burt, R. Clare, J. Ellison, J.W. Gary, G. Hanson, J. Heilman, M. Ivova PANEVA, P. Jandir, E. Kennedy, F. Lacroix, O.R. Long, A. Luthra, M. Malberti, M. Olmedo Negrete, A. Shrinivas, H. Wei, S. Wimpenny

University of California, San Diego, La Jolla, USA
J.G. Branson, G.B. Cerati, S. Cittolin, R.T. D'Agnolo, A. Holzner, R. Kelley, D. Klein, J. Letts, I. Macneill, D. Olivito, S. Padhi, M. Pieri, M. Sani, V. Sharma, S. Simon, M. Tadel, A. Vartak, S. Wasserbaech[60], C. Welke, F. Würthwein, A. Yagil, G. Zevi Della Porta

University of California, Santa Barbara, Santa Barbara, USA
D. Barge, J. Bradmiller-Feld, C. Campagnari, A. Dishaw, V. Dutta, K. Flowers, M. Franco Sevilla, P. Geffert, C. George, F. Golf, L. Gouskos, J. Gran, J. Incandela, C. Justus, N. Mccoll, S.D. Mullin, J. Richman, D. Stuart, I. Suarez, W. To, C. West, J. Yoo

California Institute of Technology, Pasadena, USA
D. Anderson, A. Apresyan, A. Bornheim, J. Bunn, Y. Chen, J. Duarte, A. Mott, H.B. Newman, C. Pena, M. Pierini, M. Spiropulu, J.R. Vlimant, S. Xie, R.Y. Zhu

Carnegie Mellon University, Pittsburgh, USA
V. Azzolini, A. Calamba, B. Carlson, T. Ferguson, Y. Iiyama, M. Paulini, J. Russ, M. Sun, H. Vogel, I. Vorobiev

University of Colorado Boulder, Boulder, USA
J.P. Cumalat, W.T. Ford, A. Gaz, F. Jensen, A. Johnson, M. Krohn, T. Mulholland, U. Nauenberg, J.G. Smith, K. Stenson, S.R. Wagner

Cornell University, Ithaca, USA
J. Alexander, A. Chatterjee, J. Chaves, J. Chu, S. Dittmer, N. Eggert, N. Mirman, G. Nicolas Kaufman, J.R. Patterson, A. Rinkevicius, A. Ryd, L. Skinnari, L. Soffi, W. Sun, S.M. Tan, W.D. Teo, J. Thom, J. Thompson, J. Tucker, Y. Weng, P. Wittich

Fermi National Accelerator Laboratory, Batavia, USA
S. Abdullin, M. Albrow, J. Anderson, G. Apollinari, L.A.T. Bauerdick, A. Beretvas, J. Berryhill, P.C. Bhat, G. Bolla, K. Burkett, J.N. Butler, H.W.K. Cheung, F. Chlebana, S. Cihangir, V.D. Elvira, I. Fisk, J. Freeman, E. Gottschalk, L. Gray, D. Green, S. Grünendahl, O. Gutsche, J. Hanlon, D. Hare, R.M. Harris, J. Hirschauer, B. Hooberman, Z. Hu, S. Jindariani, M. Johnson, U. Joshi, A.W. Jung, B. Klima, B. Kreis, S. Kwan[†], S. Lammel, J. Linacre, D. Lincoln, R. Lipton,

T. Liu, R. Lopes De Sá, J. Lykken, K. Maeshima, J.M. Marraffino, V.I. Martinez Outschoorn, S. Maruyama, D. Mason, P. McBride, P. Merkel, K. Mishra, S. Mrenna, S. Nahn, C. Newman-Holmes, V. O'Dell, K. Pedro, O. Prokofyev, G. Rakness, E. Sexton-Kennedy, A. Soha, W.J. Spalding, L. Spiegel, L. Taylor, S. Tkaczyk, N.V. Tran, L. Uplegger, E.W. Vaandering, C. Vernieri, M. Verzocchi, R. Vidal, H.A. Weber, A. Whitbeck, F. Yang, H. Yin

University of Florida, Gainesville, USA
D. Acosta, P. Avery, P. Bortignon, D. Bourilkov, A. Carnes, M. Carver, D. Curry, S. Das, G.P. Di Giovanni, R.D. Field, M. Fisher, I.K. Furic, J. Hugon, J. Konigsberg, A. Korytov, J.F. Low, P. Ma, K. Matchev, H. Mei, P. Milenovic[61], G. Mitselmakher, L. Muniz, D. Rank, R. Rossin, L. Shchutska, M. Snowball, D. Sperka, J. Wang, S. Wang, J. Yelton

Florida International University, Miami, USA
S. Hewamanage, S. Linn, P. Markowitz, G. Martinez, J.L. Rodriguez

Florida State University, Tallahassee, USA
A. Ackert, J.R. Adams, T. Adams, A. Askew, J. Bochenek, B. Diamond, J. Haas, S. Hagopian, V. Hagopian, K.F. Johnson, A. Khatiwada, H. Prosper, V. Veeraraghavan, M. Weinberg

Florida Institute of Technology, Melbourne, USA
V. Bhopatkar, M. Hohlmann, H. Kalakhety, D. Mareskas-palcek, T. Roy, F. Yumiceva

University of Illinois at Chicago (UIC), Chicago, USA
M.R. Adams, L. Apanasevich, D. Berry, R.R. Betts, I. Bucinskaite, R. Cavanaugh, O. Evdokimov, L. Gauthier, C.E. Gerber, D.J. Hofman, P. Kurt, C. O'Brien, I.D. Sandoval Gonzalez, C. Silkworth, P. Turner, N. Varelas, Z. Wu, M. Zakaria

The University of Iowa, Iowa City, USA
B. Bilki[62], W. Clarida, K. Dilsiz, S. Durgut, R.P. Gandrajula, M. Haytmyradov, V. Khristenko, J.-P. Merlo, H. Mermerkaya[63], A. Mestvirishvili, A. Moeller, J. Nachtman, H. Ogul, Y. Onel, F. Ozok[52], A. Penzo, C. Snyder, P. Tan, E. Tiras, J. Wetzel, K. Yi

Johns Hopkins University, Baltimore, USA
I. Anderson, B.A. Barnett, B. Blumenfeld, D. Fehling, L. Feng, A.V. Gritsan, P. Maksimovic, C. Martin, K. Nash, M. Osherson, M. Swartz, M. Xiao, Y. Xin

The University of Kansas, Lawrence, USA
P. Baringer, A. Bean, G. Benelli, C. Bruner, J. Gray, R.P. Kenny III, D. Majumder, M. Malek, M. Murray, D. Noonan, S. Sanders, R. Stringer, Q. Wang, J.S. Wood

Kansas State University, Manhattan, USA
I. Chakaberia, A. Ivanov, K. Kaadze, S. Khalil, M. Makouski, Y. Maravin, A. Mohammadi, L.K. Saini, N. Skhirtladze, I. Svintradze, S. Toda

Lawrence Livermore National Laboratory, Livermore, USA
D. Lange, F. Rebassoo, D. Wright

University of Maryland, College Park, USA
C. Anelli, A. Baden, O. Baron, A. Belloni, B. Calvert, S.C. Eno, C. Ferraioli, J.A. Gomez, N.J. Hadley, S. Jabeen, R.G. Kellogg, T. Kolberg, J. Kunkle, Y. Lu, A.C. Mignerey, Y.H. Shin, A. Skuja, M.B. Tonjes, S.C. Tonwar

Massachusetts Institute of Technology, Cambridge, USA
A. Apyan, R. Barbieri, A. Baty, K. Bierwagen, S. Brandt, W. Busza, I.A. Cali, Z. Demiragli, L. Di Matteo, G. Gomez Ceballos, M. Goncharov, D. Gulhan, G.M. Innocenti, M. Klute, D. Kovalskyi,

Y.S. Lai, Y.-J. Lee, A. Levin, P.D. Luckey, C. Mcginn, C. Mironov, X. Niu, C. Paus, D. Ralph, C. Roland, G. Roland, J. Salfeld-Nebgen, G.S.F. Stephans, K. Sumorok, M. Varma, D. Velicanu, J. Veverka, J. Wang, T.W. Wang, B. Wyslouch, M. Yang, V. Zhukova

University of Minnesota, Minneapolis, USA
B. Dahmes, A. Finkel, A. Gude, P. Hansen, S. Kalafut, S.C. Kao, K. Klapoetke, Y. Kubota, Z. Lesko, J. Mans, S. Nourbakhsh, N. Ruckstuhl, R. Rusack, N. Tambe, J. Turkewitz

University of Mississippi, Oxford, USA
J.G. Acosta, S. Oliveros

University of Nebraska-Lincoln, Lincoln, USA
E. Avdeeva, K. Bloom, S. Bose, D.R. Claes, A. Dominguez, C. Fangmeier, R. Gonzalez Suarez, R. Kamalieddin, J. Keller, D. Knowlton, I. Kravchenko, J. Lazo-Flores, F. Meier, J. Monroy, F. Ratnikov, J.E. Siado, G.R. Snow

State University of New York at Buffalo, Buffalo, USA
M. Alyari, J. Dolen, J. George, A. Godshalk, I. Iashvili, J. Kaisen, A. Kharchilava, A. Kumar, S. Rappoccio

Northeastern University, Boston, USA
G. Alverson, E. Barberis, D. Baumgartel, M. Chasco, A. Hortiangtham, A. Massironi, D.M. Morse, D. Nash, T. Orimoto, R. Teixeira De Lima, D. Trocino, R.-J. Wang, D. Wood, J. Zhang

Northwestern University, Evanston, USA
K.A. Hahn, A. Kubik, N. Mucia, N. Odell, B. Pollack, A. Pozdnyakov, M. Schmitt, S. Stoynev, K. Sung, M. Trovato, M. Velasco, S. Won

University of Notre Dame, Notre Dame, USA
A. Brinkerhoff, N. Dev, M. Hildreth, C. Jessop, D.J. Karmgard, N. Kellams, K. Lannon, S. Lynch, N. Marinelli, F. Meng, C. Mueller, Y. Musienko[33], T. Pearson, M. Planer, A. Reinsvold, R. Ruchti, G. Smith, S. Taroni, N. Valls, M. Wayne, M. Wolf, A. Woodard

The Ohio State University, Columbus, USA
L. Antonelli, J. Brinson, B. Bylsma, L.S. Durkin, S. Flowers, A. Hart, C. Hill, R. Hughes, K. Kotov, T.Y. Ling, B. Liu, W. Luo, D. Puigh, M. Rodenburg, B.L. Winer, H.W. Wulsin

Princeton University, Princeton, USA
O. Driga, P. Elmer, J. Hardenbrook, P. Hebda, S.A. Koay, P. Lujan, D. Marlow, T. Medvedeva, M. Mooney, J. Olsen, C. Palmer, P. Piroué, X. Quan, H. Saka, D. Stickland, C. Tully, J.S. Werner, A. Zuranski

Purdue University, West Lafayette, USA
V.E. Barnes, D. Benedetti, D. Bortoletto, L. Gutay, M.K. Jha, M. Jones, K. Jung, M. Kress, D.H. Miller, N. Neumeister, F. Primavera, B.C. Radburn-Smith, X. Shi, I. Shipsey, D. Silvers, J. Sun, A. Svyatkovskiy, F. Wang, W. Xie, L. Xu, J. Zablocki

Purdue University Calumet, Hammond, USA
N. Parashar, J. Stupak

Rice University, Houston, USA
A. Adair, B. Akgun, Z. Chen, K.M. Ecklund, F.J.M. Geurts, M. Guilbaud, W. Li, B. Michlin, M. Northup, B.P. Padley, R. Redjimi, J. Roberts, J. Rorie, Z. Tu, J. Zabel

University of Rochester, Rochester, USA
B. Betchart, A. Bodek, P. de Barbaro, R. Demina, Y. Eshaq, T. Ferbel, M. Galanti, A. Garcia-Bellido, P. Goldenzweig, J. Han, A. Harel, O. Hindrichs, A. Khukhunaishvili, G. Petrillo, M. Verzetti

The Rockefeller University, New York, USA
L. Demortier

Rutgers, The State University of New Jersey, Piscataway, USA
S. Arora, A. Barker, J.P. Chou, C. Contreras-Campana, E. Contreras-Campana, D. Duggan, D. Ferencek, Y. Gershtein, R. Gray, E. Halkiadakis, D. Hidas, E. Hughes, S. Kaplan, R. Kunnawalkam Elayavalli, A. Lath, S. Panwalkar, M. Park, S. Salur, S. Schnetzer, D. Sheffield, S. Somalwar, R. Stone, S. Thomas, P. Thomassen, M. Walker

University of Tennessee, Knoxville, USA
M. Foerster, G. Riley, K. Rose, S. Spanier, A. York

Texas A&M University, College Station, USA
O. Bouhali[64], A. Castaneda Hernandez, M. Dalchenko, M. De Mattia, A. Delgado, S. Dildick, R. Eusebi, W. Flanagan, J. Gilmore, T. Kamon[65], V. Krutelyov, R. Montalvo, R. Mueller, I. Osipenkov, Y. Pakhotin, R. Patel, A. Perloff, J. Roe, A. Rose, A. Safonov, A. Tatarinov, K.A. Ulmer[2]

Texas Tech University, Lubbock, USA
N. Akchurin, C. Cowden, J. Damgov, C. Dragoiu, P.R. Dudero, J. Faulkner, S. Kunori, K. Lamichhane, S.W. Lee, T. Libeiro, S. Undleeb, I. Volobouev

Vanderbilt University, Nashville, USA
E. Appelt, A.G. Delannoy, S. Greene, A. Gurrola, R. Janjam, W. Johns, C. Maguire, Y. Mao, A. Melo, P. Sheldon, B. Snook, S. Tuo, J. Velkovska, Q. Xu

University of Virginia, Charlottesville, USA
M.W. Arenton, S. Boutle, B. Cox, B. Francis, J. Goodell, R. Hirosky, A. Ledovskoy, H. Li, C. Lin, C. Neu, E. Wolfe, J. Wood, F. Xia

Wayne State University, Detroit, USA
C. Clarke, R. Harr, P.E. Karchin, C. Kottachchi Kankanamge Don, P. Lamichhane, J. Sturdy

University of Wisconsin, Madison, USA
D.A. Belknap, D. Carlsmith, M. Cepeda, A. Christian, S. Dasu, L. Dodd, S. Duric, E. Friis, B. Gomber, R. Hall-Wilton, M. Herndon, A. Hervé, P. Klabbers, A. Lanaro, A. Levine, K. Long, R. Loveless, A. Mohapatra, I. Ojalvo, T. Perry, G.A. Pierro, G. Polese, I. Ross, T. Ruggles, T. Sarangi, A. Savin, A. Sharma, N. Smith, W.H. Smith, D. Taylor, N. Woods

†: Deceased
1: Also at Vienna University of Technology, Vienna, Austria
2: Also at CERN, European Organization for Nuclear Research, Geneva, Switzerland
3: Also at State Key Laboratory of Nuclear Physics and Technology, Peking University, Beijing, China
4: Also at Institut Pluridisciplinaire Hubert Curien, Université de Strasbourg, Université de Haute Alsace Mulhouse, CNRS/IN2P3, Strasbourg, France
5: Also at National Institute of Chemical Physics and Biophysics, Tallinn, Estonia
6: Also at Skobeltsyn Institute of Nuclear Physics, Lomonosov Moscow State University, Moscow, Russia

7: Also at Universidade Estadual de Campinas, Campinas, Brazil
8: Also at Centre National de la Recherche Scientifique (CNRS) - IN2P3, Paris, France
9: Also at Laboratoire Leprince-Ringuet, Ecole Polytechnique, IN2P3-CNRS, Palaiseau, France
10: Also at Joint Institute for Nuclear Research, Dubna, Russia
11: Also at Zewail City of Science and Technology, Zewail, Egypt
12: Also at Helwan University, Cairo, Egypt
13: Also at British University in Egypt, Cairo, Egypt
14: Now at Ain Shams University, Cairo, Egypt
15: Also at Université de Haute Alsace, Mulhouse, France
16: Also at Tbilisi State University, Tbilisi, Georgia
17: Also at Brandenburg University of Technology, Cottbus, Germany
18: Also at Institute of Nuclear Research ATOMKI, Debrecen, Hungary
19: Also at Eötvös Loránd University, Budapest, Hungary
20: Also at University of Debrecen, Debrecen, Hungary
21: Also at Wigner Research Centre for Physics, Budapest, Hungary
22: Also at University of Visva-Bharati, Santiniketan, India
23: Now at King Abdulaziz University, Jeddah, Saudi Arabia
24: Also at University of Ruhuna, Matara, Sri Lanka
25: Also at Isfahan University of Technology, Isfahan, Iran
26: Also at University of Tehran, Department of Engineering Science, Tehran, Iran
27: Also at Plasma Physics Research Center, Science and Research Branch, Islamic Azad University, Tehran, Iran
28: Also at Università degli Studi di Siena, Siena, Italy
29: Also at Purdue University, West Lafayette, USA
30: Also at International Islamic University of Malaysia, Kuala Lumpur, Malaysia
31: Also at Malaysian Nuclear Agency, MOSTI, Kajang, Malaysia
32: Also at CONSEJO NATIONAL DE CIENCIA Y TECNOLOGIA, MEXICO, Mexico
33: Also at Institute for Nuclear Research, Moscow, Russia
34: Also at St. Petersburg State Polytechnical University, St. Petersburg, Russia
35: Also at National Research Nuclear University 'Moscow Engineering Physics Institute' (MEPhI), Moscow, Russia
36: Also at California Institute of Technology, Pasadena, USA
37: Also at Faculty of Physics, University of Belgrade, Belgrade, Serbia
38: Also at Facoltà Ingegneria, Università di Roma, Roma, Italy
39: Also at National Technical University of Athens, Athens, Greece
40: Also at Scuola Normale e Sezione dell'INFN, Pisa, Italy
41: Also at University of Athens, Athens, Greece
42: Also at Warsaw University of Technology, Institute of Electronic Systems, Warsaw, Poland
43: Also at Institute for Theoretical and Experimental Physics, Moscow, Russia
44: Also at Albert Einstein Center for Fundamental Physics, Bern, Switzerland
45: Also at Adiyaman University, Adiyaman, Turkey
46: Also at Mersin University, Mersin, Turkey
47: Also at Cag University, Mersin, Turkey
48: Also at Piri Reis University, Istanbul, Turkey
49: Also at Gaziosmanpasa University, Tokat, Turkey
50: Also at Ozyegin University, Istanbul, Turkey
51: Also at Izmir Institute of Technology, Izmir, Turkey
52: Also at Mimar Sinan University, Istanbul, Istanbul, Turkey
53: Also at Marmara University, Istanbul, Turkey

54: Also at Kafkas University, Kars, Turkey
55: Also at Yildiz Technical University, Istanbul, Turkey
56: Also at Hacettepe University, Ankara, Turkey
57: Also at Rutherford Appleton Laboratory, Didcot, United Kingdom
58: Also at School of Physics and Astronomy, University of Southampton, Southampton, United Kingdom
59: Also at Instituto de Astrofísica de Canarias, La Laguna, Spain
60: Also at Utah Valley University, Orem, USA
61: Also at University of Belgrade, Faculty of Physics and Vinca Institute of Nuclear Sciences, Belgrade, Serbia
62: Also at Argonne National Laboratory, Argonne, USA
63: Also at Erzincan University, Erzincan, Turkey
64: Also at Texas A&M University at Qatar, Doha, Qatar
65: Also at Kyungpook National University, Daegu, Korea